*Earth and Environmental Science Transactions of the Royal Society of Edinburgh*, **113**, 75–98, 2022

# Spontaneous Article

# Volcanic landscape controls on pre-rift to syn-rift volcano sedimentary systems: the Prestfjall Formation eruptive hiatus, Faroe Islands Basalt Group, northeast Atlantic

David W. JOLLEY[1]*, Simon R. PASSEY[2], Henrik VOSGERAU[3] and Erik V. SØRENSEN[3]

[1] Department of Geology & Geophysics, School of Geosciences, Meston Building, University of Aberdeen, Aberdeen, AB24 3UE, UK.
[2] Cambridge Arctic Shelf Project, West Building, Madingley Rise, Madingley Road, Cambridge, CB3 0UD, UK.
[3] Geological Survey of Denmark and Greenland, Øester Voldgade 10,1350, Copenhagen K, Denmark.
*Corresponding author. Email: d.jolley@abdn.ac.uk

ABSTRACT: The Paleogene lava flows of the Faroe Islands Basalt Group are divided into three relatively thick formations. The oldest, the Beinisvørð Formation is separated from the second lava flow succession, the Malinstindur Formation, by two formations composed primarily of volcaniclastic rocks. The oldest of these, the Prestfjall Formation has been interpreted as a period of eruptive quiescence and linked to changes in mantle melting. It is characterised in the south by the occurrence of coals, while the overlying Hvannhagi Formation is a sequence of primary and remobilised volcaniclastic strata. Field, laboratory, palynology, and photogrammetry studies have been used to investigate variations in facies and architecture within these volcaniclastic formations. The data reveal significantly different depositional systems in the Prestfjall and Hvannhagi formations over the ~40 km from the island of Vágar in the north to the island of Suðuroy in the south. Facies distribution in both the Prestfjall and Hvannhagi formations was found to have been controlled by a complex interaction of regional paleoslope, pre-existing topography, the eruption and local collapse of low-angle shield volcanoes, and minor brittle deformation. Lithological data and photogrammetry have enabled the identification of a > 180 m thick succession of volcaniclastic conglomerates deposited by lahars reworking a low-angle shield sector collapse. Co-occurrence of facies characteristic of the Prestfjall, Hvannhagi and Malinstindur formations indicate that volcanic eruption continued at a lower tempo throughout the Prestfjall Formation interval. Identification of a Beinisvørð Formation low-angle volcano shield northwest of the Faroe Islands alters the previous eruption model for this extensive lava field.

KEY WORDS: coal, isopach map, lacustrine basin, lahar, lava field, low angle shield volcano, palynology, photogrammetery, volcanic debris avalanche, volcaniclastic.

The volcanic succession of the Paleogene Faroe Islands Basalt Group (FIBG; Passey & Jolley 2009) comprises three dominantly basaltic lava flow formations separated by sedimentary rock formations (Fig. 1). The oldest lava flow succession, the Beinisvørð Formation, comprises a thick succession of simple, sheet-like, lava flows (Passey & Bell 2007; Passey & Jolley 2009). The exposed succession shows an increase in the dominance of columnar jointing towards the top, including thick multi-tiered columnar jointed flows in central east Suðuroy. The Malinstindur Formation is a thick succession of dominantly compound lava flows which is separated from the Beinisvørð Formation by two volcano–sedimentary rock formations (Passey & Bell 2007; Passey & Jolley 2009). The oldest of these, the Prestfjall Formation, is composed of carbonaceous and dominantly argillaceous sedimentary rocks (Passey & Jolley 2009) which crop out most extensively on the island of Suðuroy (Rasmussen & Noe-Nygaard 1970). The formation is generally poorly exposed and has been mainly characterised by observations made from the coal mines on Suðuroy (Rasmussen & Noe-Nygaard 1970). To the north, the Prestfjall Formation crops out on the islands of Tindhólmur and western Vágar (Fig. 1), but is of a notably more arenaceous character. The lower boundary of the Prestfjall Formation has been interpreted to mark a significant hiatus in volcanic activity following the cessation of Beinisvørð Formation eruptions (Rasmussen & Noe-Nygaard 1970). Overlying the Prestfjall Formation, the volcaniclastic rocks of the Hvannhagi Formation crop out in eastern Suðuroy, at isolated locations in north-west Suðuroy, west Vágar, and on Tindhólmur. The formation comprises both pyroclastic and volcaniclastic sedimentary rocks that were deposited in a terrestrial environment (Passey & Jolley 2009), and has been regarded as marking the resumption of large-scale volcanism in the region (Passey 2004).

Recent analysis of upper Beinisvørð Formation lava flow geochemistry (Millett *et al.* 2020) has provided evidence for both an increase in the overall degree of partial melting and a reduction

© The Author(s), 2022. Published by Cambridge University Press on behalf of The Royal Society of Edinburgh. This is an Open Access article, distributed under the terms of the Creative Commons Attribution licence (http://creativecommons.org/licenses/by/4.0/), which permits unrestricted re-use, distribution, and reproduction in any medium, provided the original work is properly cited. doi:10.1017/S1755691022000056

https://doi.org/10.1017/S1755691022000056 Published online by Cambridge University Press

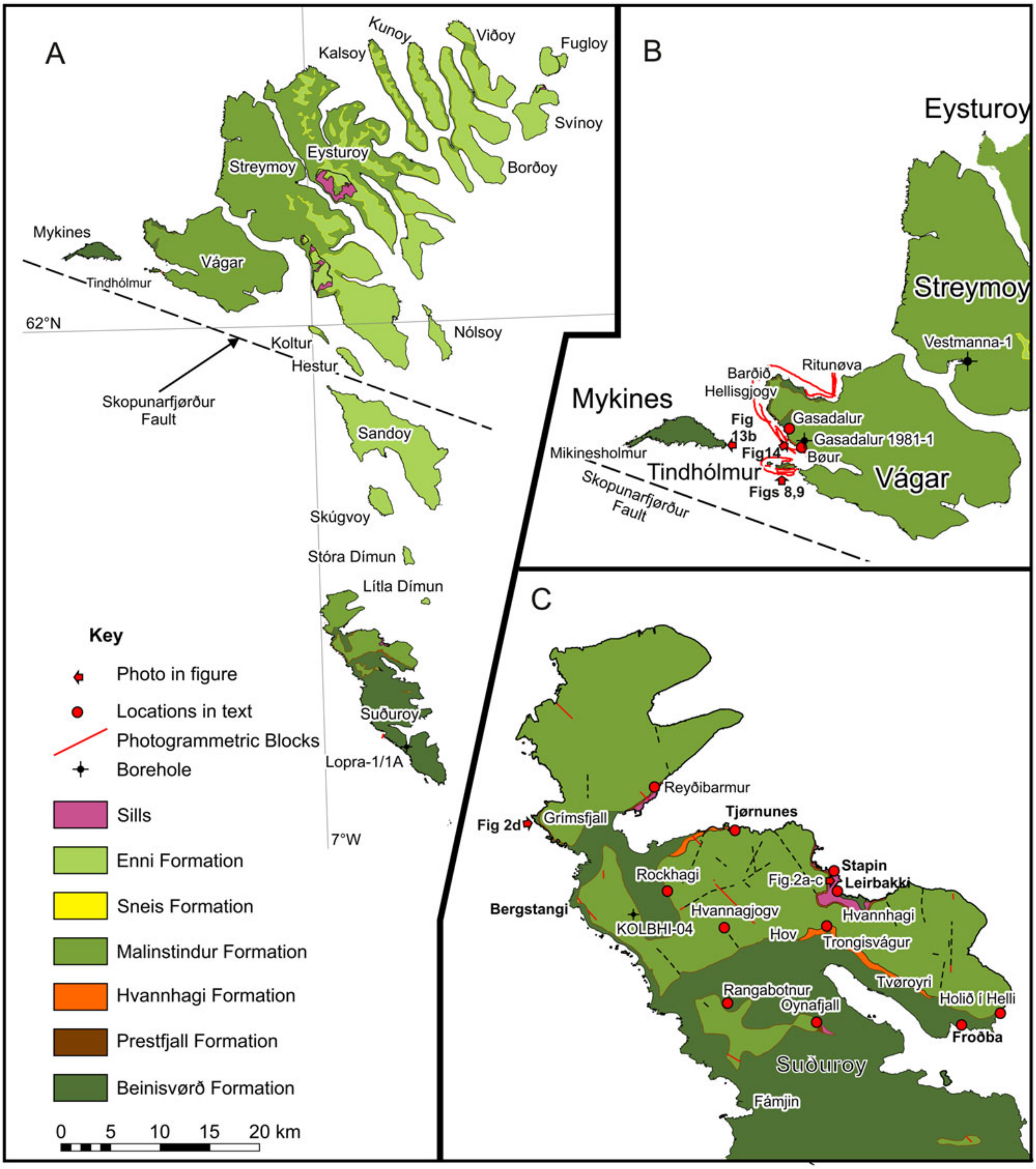


**Figure 1** Simplified geology and location map of the Faroe Islands Basalt Group (a). Maps B and C show larger scale maps of the two key geographical areas, Vágar, Tindhólmur and Mykines (b) and northern Suðuroy (c).

in the initial pressure of melting. An increase in partial melting was identified from data recorded in lava flows from the upper Beinisvørð Formation. This was interpreted as evidence for the early onset of northeast Atlantic rifting. Millett *et al.* (2020) also proposed a linkage between the reduction in initial pressure of melting, a transient reduction in mantle temperature, and the North Atlantic Igneous Province (NAIP) wide volcanic hiatus. This was correlated with a proposed increase in thickness and duration of interbedded sedimentary rock units prior to cessation of volcanism and deposition of the carbonaceous Prestfjall Formation.

Attributed to the transition from pre-rift to syn-rift (Larsen *et al.* 1999; Millett *et al.* 2020), FIBG strata between the extrusive successions of the Beinisvørð and Malinstindur formations are stratigraphically complex and spatially variable. This study contributes to the understanding of this complexity which will help to answer questions regarding the rate of slowing, cessation, and resumption of eruption at a period of major reorganisation of the NAIP.

## 1. Methods

### 1.1 Photogrammetry and field data collection

Primary lithological records were collected from outcrops in the field. Field transects and spot locations were recorded (Vágar and Suðuroy) and borehole core was logged from Suðuroy (KOLBH1-04) and Vágar (Gásadalur 1989-1). Many of these

https://doi.org/10.1017/S1755691022000056 Published online by Cambridge University Press

are detailed in Passey & Jolley (2009), but are supplemented here with additional data. Lithology, structure, and thickness of rock units were used to construct maps, with photogrammetry interpretation undertaken on models for cliff sections from Vágar and Tindhólmur. The photogrammetry models were prepared following the workflow described in Passey *et al*. (2016), Vosgerau *et al*. (2016), and Sørensen & Dueholm (2018). Briefly summarised, stereo-images (overlapping images) of the coastal cliffs were acquired using a single handheld digital camera deployed on a helicopter flying with an open door. The camera was pointed approximately perpendicular to the slope of the cliffs and the pilot was instructed to fly parallel to the cliffs. The images were prepared for analysis using the Agisoft software Metashape for tie-point generation. The triangulation or bundle adjustment of the images were then undertaken in the Anchorlab software three-dimensional (3D) Stereo Blend using a combination of the tie-points, Global Positioning System data, sea-level levering points, and control points taken from the Faroes Environment Agency online portal (www.kortal.fo). The orientation of the images (results of the triangulations) was exported from 3D Stereo Blend and used to generate 3D mesh models of the cliff phases using nFrames software SURE. These, which in the following will be referred to as the photogrammetry models, were subsequently interpreted using Lime v2.2.1. (Buckley *et al*. 2019). Photogrammetry models were interpreted with cross-reference to air, boat, and shore photographs to clarify details. The models were interpreted using colour-coded lines to characterise different volcanic and sedimentary beds. More laterally extensive surfaces (e.g., large flow unit tops and unconformities) were highlighted to allow for tracing depositional packages. These extensive surfaces together with some indicative bed junctions were then exported and are presented here. Surface co-ordinates for significant facies changes and unconformities were exported into a spreadsheet and then to Surfer10 to create surface and isochron maps.

## 1.2 Palynology

Samples were taken for palynological analysis from shales, coals, and poorly sorted sandstone units in field sections and from cored boreholes. These were processed following standard techniques, including hydrofluoric acid digestion, boiling in 20% hydrochloric acid to remove precipitates, and oxidation for 5 min in dilute 40% nitric acid where necessary. Coal samples were prepared by dissolution using fuming nitric acid. The resultant >7 μm residues were mounted in a permanent petropoxy mounting medium and examined under a transmitted light Olympus BX53 microscope. For each sample, counts of 250 specimens were targeted, but with the highly variable recovery from interlava field sedimentary rocks, frequently not attained. Accordingly, data are normalised as percentages in sections where larger counts were obtained, and as square roots in more variable recovery sections.

Ecological analysis of palynological data was used to underpin depositional environment interpretations of sedimentary rocks. Many terrestrial sedimentary sequences demonstrate progression in plant community seral succession through the duration of their deposition; these stages of community ecology are referred to as early, mid, and late successions (e.g., Vitousek 2004; Jolley *et al.* 2009). Within the NAIP, newly erupted lava flow surfaces and volcaniclastic sediment deposits would, with the passage of time, begin to be colonised by early successional plant communities. These were dominated by disturbance and stress tolerant species (e.g., *Equisetum*, 'mares' tails') and in humid environments, ferns, and mosses. In the absence of disturbance, these communities would have diversified to form early–mid successional communities (Whittaker *et al*. 1989; Thornton 2000). Palynofloras derived from these communities were dominated by polypodiaceous fern spores (e.g., *Laevigatosporites haardtii*), but include moss and liverwort spores, *Ginkgo* pollen (*Monocolpopollenites tranquilus*), and walnut/hickory pollen (Juglandaceae; *Caryapollenites*, *Momipites* and *Platycaryapollenites* species). In Miocene and younger volcanic terrains, primary succession has involved grasses and herbaceous angiosperms as key early colonists (Whitaker *et al*. 1989; Thornton 2000). Evidence indicates that this niche was dominated by ferns in the Paleogene (Jolley 1997; Jolley *et al*. 2009).

Continuing substrate stability over time would have led to the development of mid-successional vegetation. Palynofloras derived from these communities are higher in diversity, and are typified by Fagaceae (chestnut types), Platanaceae (plane types) Juglandaceae (walnut and hickory types) and Myricaceae (myrtles and hazel types). Many of these taxa occur within other communities, but at lower frequencies. Fagaceous pollen attributed to *Cupuliferoipollenites*, which is one of the dominant taxa in this grouping, occur in a wide variety of assemblages but decline in significance in late successional vegetation.

Late successional vegetation within the NAIP was most often dominated by a Cupressaceae–Nyssaceae association (swamp cypress and black gum), which is of low diversity (e.g., Jolley *et al*. 2009, 2012). This community often formed the climax vegetation. A number of species important in early–mid and mid successional vegetation decline in importance and diversity in this community as they were eliminated by effective competition from Cupressaceae–Nyssaceae mire species. Patchworks of disturbed areas within this late-successional community are inferred from the incursion of other species; these include the taxon *Caryapollenites*, which is associated with mid-successional mires (Ellis *et al*. 2009; Jolley *et al*. 2009). Other such taxa, including *Monocolpopollenites tranquilus* (*Ginkgo*), *Retitricolpites retiformis* (Platanaceae) and *Tricolpites cf. hians* (Platanaceae), have previously been noted as part of riparian vegetation groupings (Streigler 1990; Jolley 1997), characteristic of disturbed fluvial margin environments. Accompanying these species was a range of taxa of lesser significance that may represent disturbed vegetation or understory.

Distributed across the range of environments is the betulaceous grain *Alnipollenites verus*. This taxon has been suggested as a nitrogen-fixing early colonist in nutrient depleted soils (Chapin *et al*. 1994; Hobbie *et al*. 1998; Jolley *et al*. 2008). Its occurrence suggests that the soils were nutrient deficient across a range of profiles.

In addition to pollen and spores from higher plants, the palynofloras recovered from the FIBG include green algae, acritarchs, and dinoflagellate cysts. Chlorophycean algae occur commonly in samples from lava field sedimentary rock interbeds, where they are indicative of bodies of low-energy fresh to weakly brackish water. Small acanthomorph acritarchs are recovered frequently from tidally influenced fluvial deposits (Jolley *et al*. 2012, 2021), where they probably tolerated weakly saline water masses. Dinoflagellate cysts have been recorded from a range of normal salinity marine and brackish water environments in the Paleogene (e.g., Bujak *et al.* 1980; Pross & Brinkhuis 2005; Vieira & Jolley 2020), following similar distribution patterns to those of extant species. However, the small size of these palynomorphs means that they behave as silt size sedimentary particles in depositional systems. This taphonomic factor is reflected in their low frequency occurrence within the tidal limit of estuarine systems.

The palynological taxonomy used in this study is that of dinoflaj3 (dinoflagellate cysts), Tappan (1980; other algae), and Jolley & Morton (1992; pollen and spores).

## 1.3 Whole rock geochemistry

A limited study of major and trace element geochemistry of the cored sedimentary interbeds was conducted using X-ray

https://doi.org/10.1017/S1755691022000056 Published online by Cambridge University Press

fluorescence (XRF) and flame atomic absorption photospectrometry (FAAS). Samples collected for palynology were analysed for major element geochemistry with some trace element analysis. Standard XRF techniques were used to analyse the range of major oxides and trace elements present (see Supplementary data S1 and S2; available at: https://doi.org/10.1017/tre2200005). These data are presented either as element oxide ratios or as major element weathering indices (Sheldon & Tabor, 2009). Ratios and indices are correlated to palynology-derived plant community ecology and changes in the depositional system to highlight links to depositional system dynamics and plant nutrient uptake (Vitousek, 2004; Jolley *et al.,* 2008, 2012).

## 2. Pre-rift to syn-rift rock succession on Suðuroy

The Prestfjall and Hvannhagi formations of the island of Suðuroy have received the majority of attention from past scientific studies. This was principally because of the lithological evidence that the carbonaceous sediments presented for a major hiatus in FIBG eruption, but also for the resource implications of the coal beds. The current study initially focusses on the Prestfjall and Hvannhagi formations of Suðuroy within the context of this published research. This research is expanded by the addition of palynological and contextual lithological evidence from previously unstudied exposures and boreholes. Integration of these new data with the published record has allowed understanding of the processes controlling deposition of both the Prestfjall and Hvannhagi formations in Suðuroy. From this data-rich geographical area, the current study extends the understanding of these important interlava units into the little studied northerly exposures of Tindhólmur and Vágar.

### 2.1. Prestfjall Formation

On Suðuroy, the Prestfjall Formation covers an area of ~23 km$^2$ and where complete, ranges in thickness between 3 m and 15 m with an average thickness of ~9 m (Rasmussen & Noe-Nygaard 1970). The Beinisvørð–Prestfjall Unconformity (Passey & Varming 2010) exhibits some incision into the uppermost flows of the Beinisvørð Formation and is overlain by the sedimentary rocks of the Prestfjall Formation (Passey & Jolley 2009). The Prestfjall Formation (Fig. 2d) is usually only accessible and exposed in completeness in mine workings, which except for one on the east side of the Rokhagi valley are now all closed. Fortunately, a complete description of the Prestfjall Formation derived from now closed mine workings and test pits was made by Rasmussen & Noe-Nygaard (1970), who described 41 separate profiles from the island of Suðuroy (Supplementary Data S3).

These authors also subdivided the Prestfjall Formation into 5–6 informal beds based on the position of two commonly occurring coal seams (Rasmussen & Noe-Nygaard 1970). The combined coal seam thickness rarely exceeded 1 m, having an average thickness of between 70 cm and 80 cm (Rasmussen & Noe-Nygaard 1970; Lund 1989), although an exceptional thickness of ~1.7 m was observed locally (Lund 1989). The base of the Prestfjall Formation is commonly composed of a whitish-grey ‘underclay’ that has a maximum thickness of ~1 m (Rasmussen & Noe-Nygaard 1970). However, in profiles examined here, KOLBH1-04 borehole and Holið í Helli (Fig. 1), the ‘underclay’ is represented by a sideritic claystone succession with a thickness of 4 m–10 m (Passey 2014).

The ‘underclay’ bed is usually overlain by the ‘lower coal’, which has an average thickness of between 38 cm and 45 cm, and a maximum thickness that rarely exceeds 1 m (Rasmussen & Noe-Nygaard 1970). The coal of the lower coal seam is usually composed of alternating layers of dull (durain) and bright (vitrain) coal. The lower coal seam is commonly overlain by a dark shale that has an average thickness of ~24 cm, and which frequently contains streaks and lenses of bright (vitrain) coal (Rasmussen & Noe-Nygaard 1970; Passey 2014). The upper coal seam overlies the dark shale and has an average thickness of ~38 cm, and a maximum thickness in the region of ~80 cm (Rasmussen & Noe-Nygaard 1970; Passey 2004). The coal seam is commonly composed of bright (vitrain) coal.

The ‘upper coal’ is generally overlain by the ‘roof clay’ that reaches a maximum observed thickness of ~13 m (Rasmussen & Noe-Nygaard 1970), and is locally termed ‘ranin’. The lower part of the roof clay sometimes contains streaks or lenses of coal (Passey 2014). The upper part is locally a reddish claystone unit, informally referred to as ‘takleir’. At several locations in western Suðuroy the ‘ranin’ roof clay is incised by channels containing greenish-brown volcaniclastic sandstones and granule-grade conglomerates with an observed maximum thickness of ~4 m (Rasmussen & Noe-Nygaard 1970; Passey 2004). The volcaniclastic sandstones are composed of palagonitised basaltic glass with a large proportion, particularly in the conglomerates, of finely crystalline basalt clasts of various compositions and textures.

### 2.2. Hvannhagi Formation

The lower rock units of the Hvannhagi Formation on Suðuroy comprise a sequence of air-fall tuffs and lapillistone fall deposits at least 25 m thick, or a succession of volcaniclastic conglomerates up to 8 m in thickness (Passey & Jolley 2009). An accurate thickness for these units is difficult to obtain because of thick, irregular dolerite sills, particularly in the northeast of Suðuroy (Fig. 2a, c). The pyroclastic sequence of greyish to red (where weathered) coarse tuffs and lapillistones are overlain by a 3 m–17 m thick sequence of volcaniclastic mudstones, sandstones, and conglomerates. These volcaniclastic sedimentary rocks are immature and are predominantly composed of reworked palagonitised basaltic glass clasts with rare clasts of finely crystalline basalt. Occasionally, reworked clasts of the underlying greyish olivine-phyric coarse tuff are observed within this sequence. Locally, this 3 m–17 m thick volcaniclastic sedimentary section contains a heterolithic unit of thinly-bedded sandstones and mudstones up to 5.5 m thick (Fig. 2b).

This volcaniclastic sedimentary succession is overlain by a 1 m–4 m thick greyish olivine-phyric welded tuff (Passey & Jolley 2009). The coarse tuff is homogeneous and contains abundant elongated dark brown flattened fiamme, which define a planar foliation or eutaxitic texture (Passey 2004). The tuff is, in turn, overlain by a 1 m–9 m thick sequence of poorly sorted volcaniclastic sedimentary conglomerates and sandstones, composed dominantly of reworked palagonitised basaltic glass clasts. Other clasts are composed of coal, volcaniclastic mudstone, finely crystalline basalt, and olivine-phyric tuff.

### 2.3 New palynological observations on the Prestfjall and Hvannhagi formations, Suðurøy

Records of the Prestfjall Formation succession in exposures and mine workings were made by Rasmussen & Noe-Nygaard (1970); these focussed principally on their value as a coal resource. These records have been supplemented by additional field sections and a borehole (KOLBH1-04, Fig. 1c).

**2.3.1. Holið í Helli profile.** The Holið í Helli profile in northeast Suðuroy (Fig. 3) was described in detail by Passey (2014). Overlying the Beinisvørð Formation basaltic lava flows and a post-Prestfjall Formation sill are <4 m of volcaniclastic sandstones and conglomerates which are, in turn, overlain by >4 m of clay ironstone. The uppermost beds of the Prestfjall Formation comprise 5.5 m of nodular mudstone, bright coal, and organic-rich mudstone. A sharp and planar contact separates the Prestfjall Formation from the overlying 3 m thick sequence

https://doi.org/10.1017/S1755691022000056 Published online by Cambridge University Press

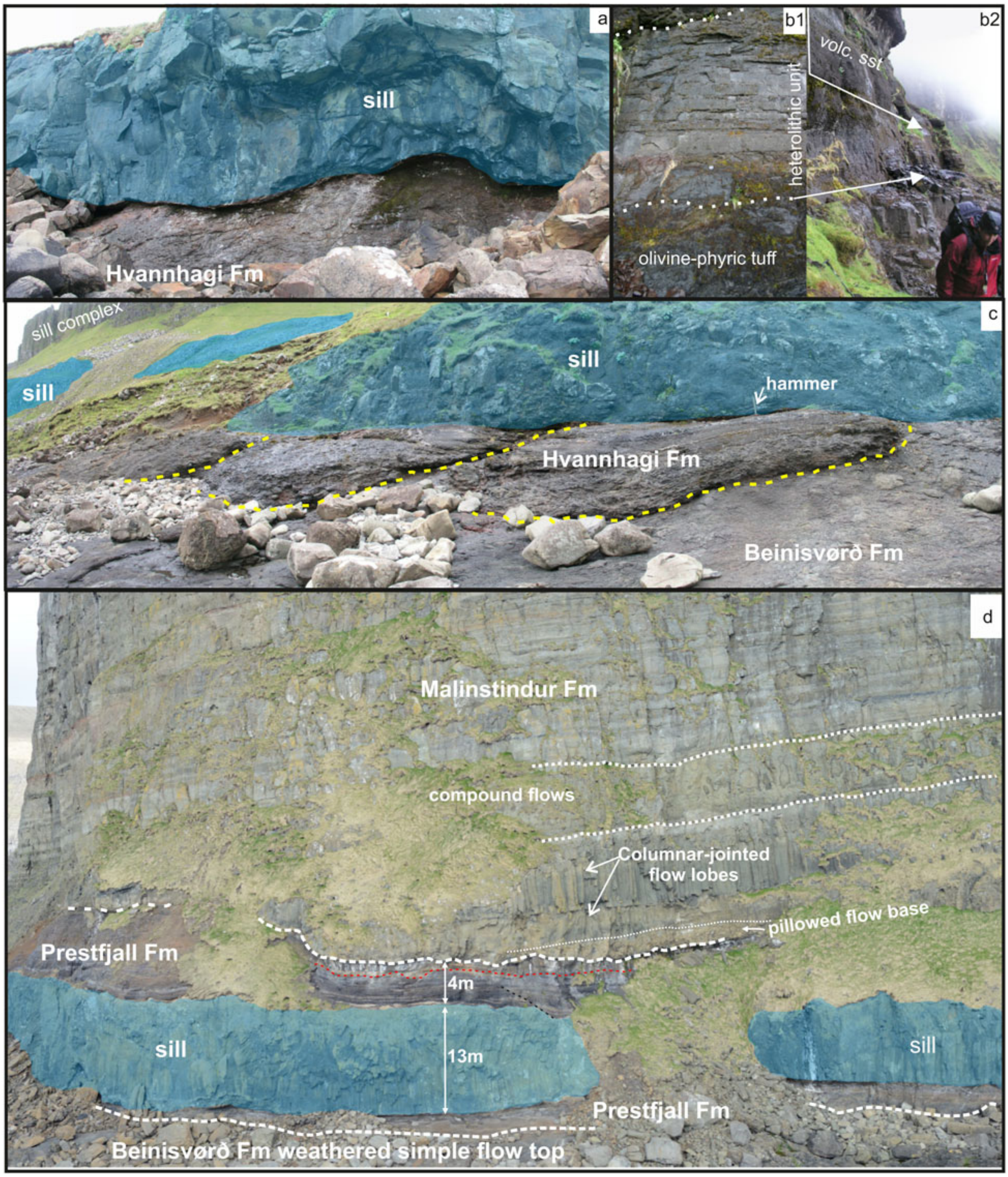


**Figure 2** Interpreted field photographs of: (a, c) the basal Hvannhagi Formation at Leirbakki, northeast Suðuroy, composed of poorly sorted conglomerates in lobate beds (hammer for scale in (c); (b) heterolithic Hvannhagi Formation volcaniclastic sandstones at Hvannhagi, northeast Suðuroy (lens cap for scale in b1; person for scale in b2); (d) cliffs at Grímsfjall, Suðuroy showing the Prestfjall Formation hosting large sills with intrusive finger lobes (Schofield *et al*. 2012). A post-Prestfjall eroded channel was filled by ponded, columnar jointed Malinstindur Formation flows. These are in turn overlain by characteristic compound flows of the Malinstindur Formation. Intrusive basaltic sills are shaded in transparent blue for clarity.

of devitrified tuff beds attributed to the Hvannhagi Formation (Passey 2004, 2014).

Palynological analysis of a suite of samples from the Prestfjall Formation at this exposure yielded palynofloras completely dominated by septate fungal hyphae, with rare occurrences of gymnosperm pollen (Fig. 3). An abrupt change in the character of the assemblages was recorded above 10 m from the base of the section, within the clay ironstone bed (Fig. 3). Samples above this level are largely barren of palynomorphs, which given the nature of the organic rich mudstone is noteworthy, possibly reflecting oxidation of organic matter *in situ*. A single sample at the top of the organic-rich mudstone (Bed 6, Fig. 3) yielded a palynoflora including swamp cypress pollen (*Inaperturopollenites hiatus*), the juglandaceous angiosperm pollen *Caryapollenites circulus*, and the early successional pteridophyte spore *Laevigatosporites haardtii*. This assemblage is indicative of early–mid succession vegetation growing within the catchment, but transported into the lacustrine depositional environment (Jolley *et al*. 2009).

https://doi.org/10.1017/S1755691022000056 Published online by Cambridge University Press

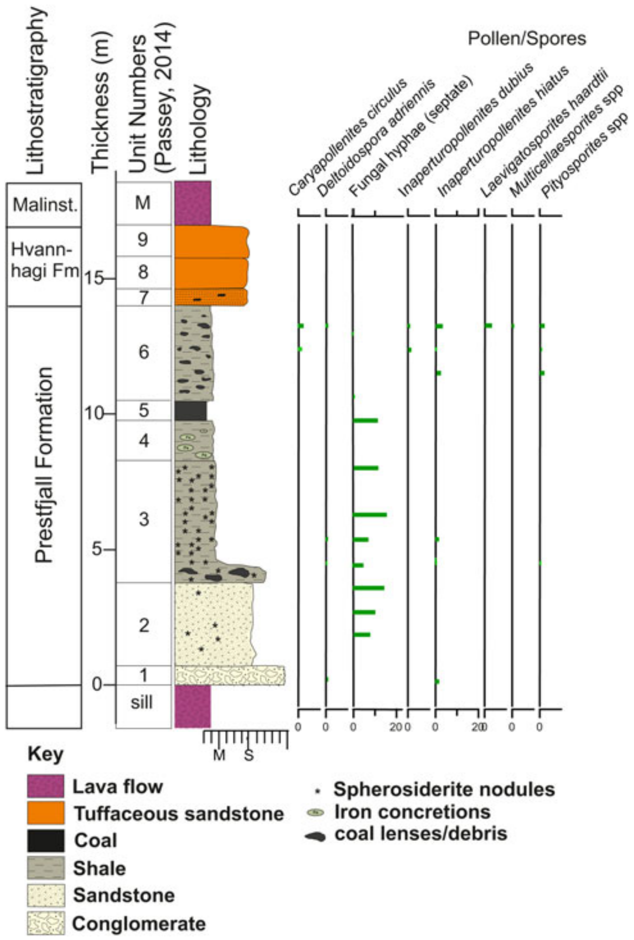


**Figure 3** Holið í Helli profile. Depositional units are those of Passey (2014). Because of variable abundances of palynomorphs in each sample, the selected palynology data are plotted as square roots.

Variations in clay ironstone facies were used by Passey (2014) to demonstrate that the Prestfjall Formation at Holið í Helli was deposited in a shallow lacustrine environment. The absence of rootlets in the succession indicates that the shallow lacustrine facies did not become emergent at any time, although Passey, (2014) suggested that oxidation rims in siderite spherules indicated seasonal water depth variations. Deposition in a shallow lava field lake is supported by the palynological data, accumulations of fungal debris being characteristic of lacustrine environments in Cenozoic lava fields (Jolley *et al.* 2009). The low diversity, early–mid succession flora of Bed 6 (Fig. 3) is interpreted as having been deposited in a proximal, shallower lake. Subsequent pyroclastic activity forming the oldest units of the Hvannhagi Formation resulted in interaction of tephra with the Prestfjall Formation-lake, leading to devitrification and the layering of the oldest of the three tuffaceous units. From the evidence available at the Holið í Helli location, it is not possible to determine unequivocally if the onset of pyroclastic activity caused a cessation to lacustrine carbonaceous sediment deposition. However, the presence of common allochthonous petrified wood fragments in the oldest tuffaceous bed (Bed 7, Fig. 3) indicates that deposition of the Prestfjall Formation lacustrine sediments was potentially coeval with the onset of Hvannhagi Formation pyroclastic activity. Reworking of these wood fragments into the Hvannhagi Formation from older Prestfjall Formation strata is thought unlikely, as there is no accompanying coal or volcaniclastic siltstone lithoclasts recorded in Bed 7.

**2.3.2. Rokhagi mine section.** This section was recorded and palynology samples collected in an active mine adit in 1997, where the working exposed a section similar to that recorded by Lund (1983, 1989) and Parra *et al.* (1987), although the basal part of the 'underclay' and the 'roof clay' were not exposed (Fig. 4). Palynofloras from samples taken from the 'underclay' were dominated by the swamp cypress pollen *Inaperturopollenites hiatus*, with few *Pityosporites* (Pinaceae). *Inaperturopollenites hiatus* is abundant in many interbed successions, the parent Cupressaceae, swamp cypress plants being pollen overproducers, resulting in the taxon occurring abundantly in a range of flow top and floodplain depositional environments in lava fields (Jolley 1997; Jolley *et al.* 2009). The rest of the 'underclay' assemblage is diverse with low taxon dominance. Assemblages include floodplain fern-derived pteridophyte spores (*Deltoidospora*), juglandacous angiosperm pollen (*Momipites* species and *Caryapollenites* species), and *Alnipollenites verus* (Betulaceae and *Alnus* types). These were derived from a mid-seral succession transitional swamp plant community (Jolley *et al.* 2009, 2015), indicating longer-term substrate stability within the catchment area. Occurrences of the chlorophycean algae *Botryococcus braunii*, indicate deposition in a freshwater lacustrine environment (Tappan 1980).

The overlying dull coal unit lacks a leached seat earth and has no preserved root structures. It yielded a diverse palynoflora of similar composition to the 'underclay'. The common wetland angiosperm pollen, *Alnipollenites verus* declines in abundance up section, with *I. hiatus* becoming dominant. Dominance of this swamp cypress pollen overproducer is characteristic of distal lacustrine facies (Jolley *et al.* 2009; Daly *et al.* 2011a). This lower, fusain rich coal is separated from the upper vitrain rich bright coal by a thin grey shale unit ('mid clay'), again with no root traces present. The lower 'mid clay' is dominated by *Laevigatosporites haardtii*, spores derived from a primary colonist pteridophyte fern. These ferns were common at riparian fluvial margins and disturbed forested areas (Collinson 2002; Jolley *et al.* 2009; Daly *et al.* 2011a). In the upper part of the 'mid-clay' these fern spores are replaced by a diverse angiosperm pollen flora, which includes *Momipites* spp., *Caryapollenites circulus*, and *C. veripites* (Fig. 5). These taxa were derived from juglandaceous angiosperms, characteristic of early mid-successional vegetation swamp communities (Wing & Hickey 1984; Jolley *et al.* 2009; Daly *et al.* 2011b). Samples from the 'upper coal' are totally dominated by swamp cypress pollen (*I. hiatus*) in low diversity, allochthonous assemblages.

Occurrences of the acritarch *Chomotriletes* and the chlorophycean algae *Schizosporis parvus* are indicative of waterlogged soils and lacustrine biofacies (Tappan 1980). These algae, the lack of root fossils, the absence of soil profiles, and the dominance of swamp cypress pollen in low diversity assemblages support interpretation as a lacustrine depositional environment (Lund 1989; Passey 2014). This interpretation is further supported by the finely laminated nature of the Prestfjall Formation units at exposure (Fig. 4a). Within the lacustrine basin, the durain and fusain rich coals were formed from concentrations of drifted plant material, although dispersed woody plant material occurred in the majority of lithological units.

Although >2 m of the 'roof clay' was sampled in the Rokhagi mine exposed faces, the palynofloras show a similar, apparently seral successional trend to that recorded in the underlying 'mid clay' to 'upper coal' interval. Primary successional fern dominated (*Laevigatosporites haardtii*) assemblages were replaced by diverse, angiosperm pollen (dominantly *Momipites* and *Caryapollenites* species) rich palynofloras (Figs 4, 5). These were in turn succeeded by palynofloras wholly dominated by swamp cypress pollen (*I. hiatus*). These repeated apparent seral

https://doi.org/10.1017/S1755691022000056 Published online by Cambridge University Press

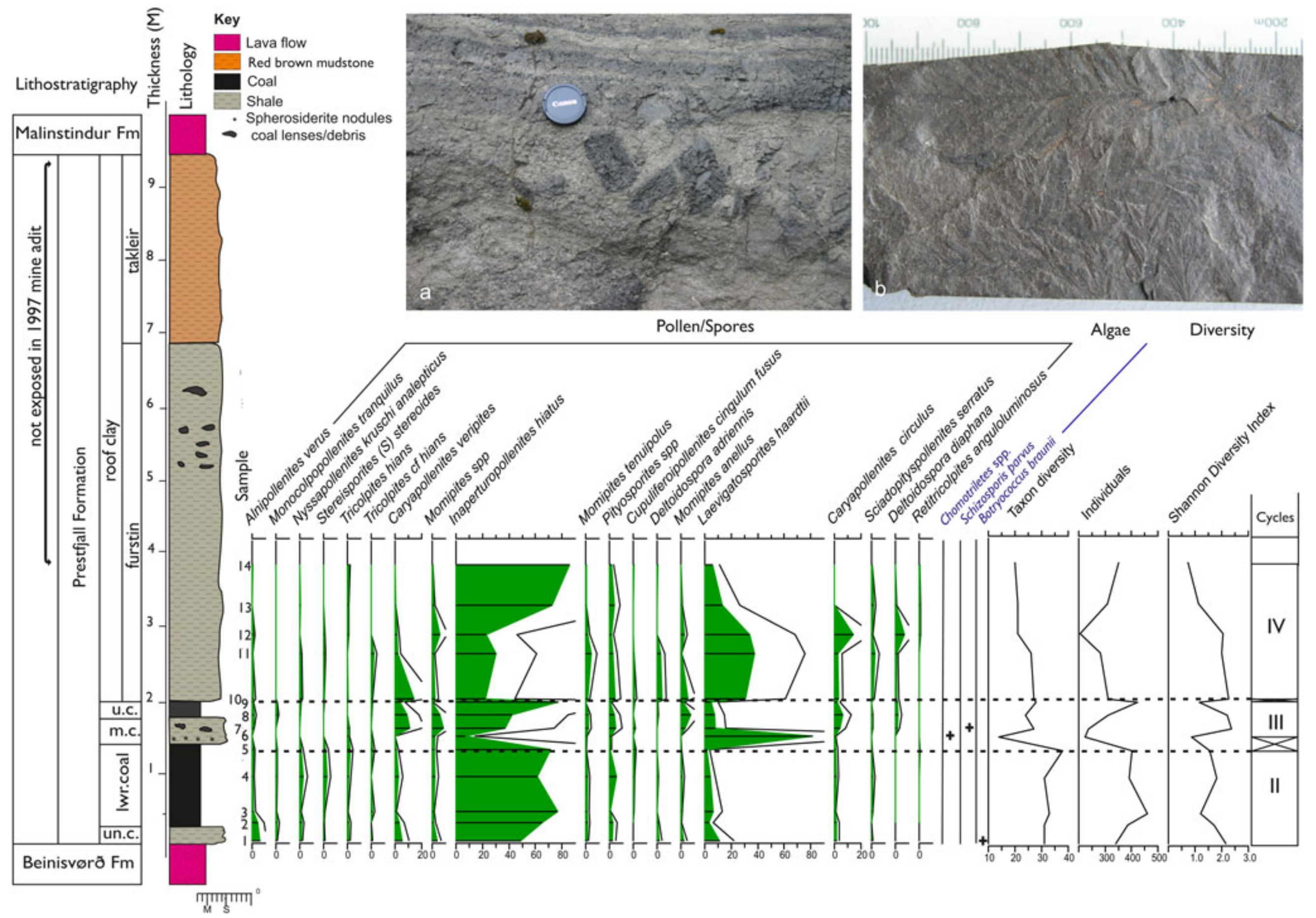


**Figure 4** Rokhagi mine profile and palynology data plotted as percentages of the total palynoflora. Note that the section above 4 m was not exposed in the workings at the time of sample collection. Lithology abbreviations, un.c. = 'underclay'; m.c. ='mid clay'; u.c. = 'upper coal'. Photographs show (a) fine laminated bedding in the Prestfjall Formation of sill-rafted block from the Stapin area (lens cap for scale); (b) specimen of the macrofossil *Metasequoia occidentalis* (Newberry) Chaney, 1951. This plant produced pollen of the type recorded as *Inaperturopollenites hiatus* in the diagram below (specimen held in collection of Jarðfeingi, Tórshavn).

succession trends reflect increasing distance from the input point to the lacustrine system and potentially, increased lake water depth.

**2.3.3. KOLBH1-04 borehole.** The KOLBH1-04 borehole [61.56888N, 6.93527W] was drilled in 2004 on the west side of the Rokhagi valley to test coal reserves away from the then open mines on the eastern side of the valley (Fig. 1). A number of thin coaly intervals occur in the lower ~7 m of the Prestfjall Formation, which overlie an aphyric basalt lava flow of the Beinisvørð Formation. There is no differentiated 'underclay' although the named coal units of Rasmussen & Noe-Nygaard (1970) were identified at the time of drilling (Fig. 6). The 'roof clay' unit of the Prestfjall Formation is overlain by the Hvannhagi Formation consisting of 0.6 m of volcaniclastic sandstone succeeded by 0.3 m of peperite beneath the overlying olivine-phyric flows of the Malinstindur Formation lava flow field. The red-brown mudstones of the 'takleir' unit of the roof clay are not present in this borehole although it is <0.5 km from the Rokhagi mine adits.

Palynofloras recovered from this succession are similar to those recorded in the Rokhagi mine section (Fig. 4). All were dominated by *I. hiatus* (Cupressaceae, *Taxodium*) and *Pityosporites* spp. (Pinaceae, pines) associated with common occurrences of *Caryapollenites circulus* (Juglandaceae, *Carya*) and *Laevigatosporites haardtii* (a primary colonist polypodiaceous fern). These taxa are associated with frequently occurring *Caryapollenites* species (*C. veripites, C. inelegans* and *C. triangulus*, see Figs 5, 6), and fagaceous pollen (*Cupuliferoipollenites cinglum* and *Cupuliferoidaepollenites liblarensis*). In the KOLBHI-04 borehole, these more diverse assemblages were recovered from four separate intervals within the Prestfjall Formation succession (Fig. 6).

Samples taken at 217.4 m, 218.7 m, and 219.0 m all yielded marine dinoflagellate cysts including *Areoligera cf. coronata* and *A. cf. senonensis* (Fig. 6) associated with brackish to freshwater acritarchs and chlorophycean algae (*Pediastrum bifidites*, *Botryococcus braunii*, *Schizosporis parvus* and *Leiosphaeridia* spp.). The dinoflagellate cysts in this assemblage are often associated with shallow marine sediments, particularly shoreface deposits (Pross & Brinkhuis 2005; Jolley *et al.* 2021). Because they behave as silt-size sedimentary particles, they are prone to transportation by tidal action within tidally influenced fluvial channel depositional systems to the extent of the tidal limit (Anderson 1998; Debenay *et al.* 2003).

At the upper boundary of this microplankton bearing interval are occurrences of spores and pollen reworked from older sedimentary rocks (Fig. 6). These taxa indicate reworking of Carboniferous, Triassic, and Late Cretaceous palynofloras and transportation into the FIBG lava field, probably within lithoclasts.

FAAS analysis was conducted on the same sample set used for palynological analysis. Attention was focussed on relative trends within the FAAS data, particularly ratios which highlight volcaniclastic input and weathering (Retallack 1999; Sheldon, 2003; Jolley *et al.* 2008; 2012). Both the barium:strontium (Ba:Sr), and aluminium:phosphate ratios measured mobile element loss through weathering and plant uptake (Vitousek

https://doi.org/10.1017/S1755691022000056 Published online by Cambridge University Press

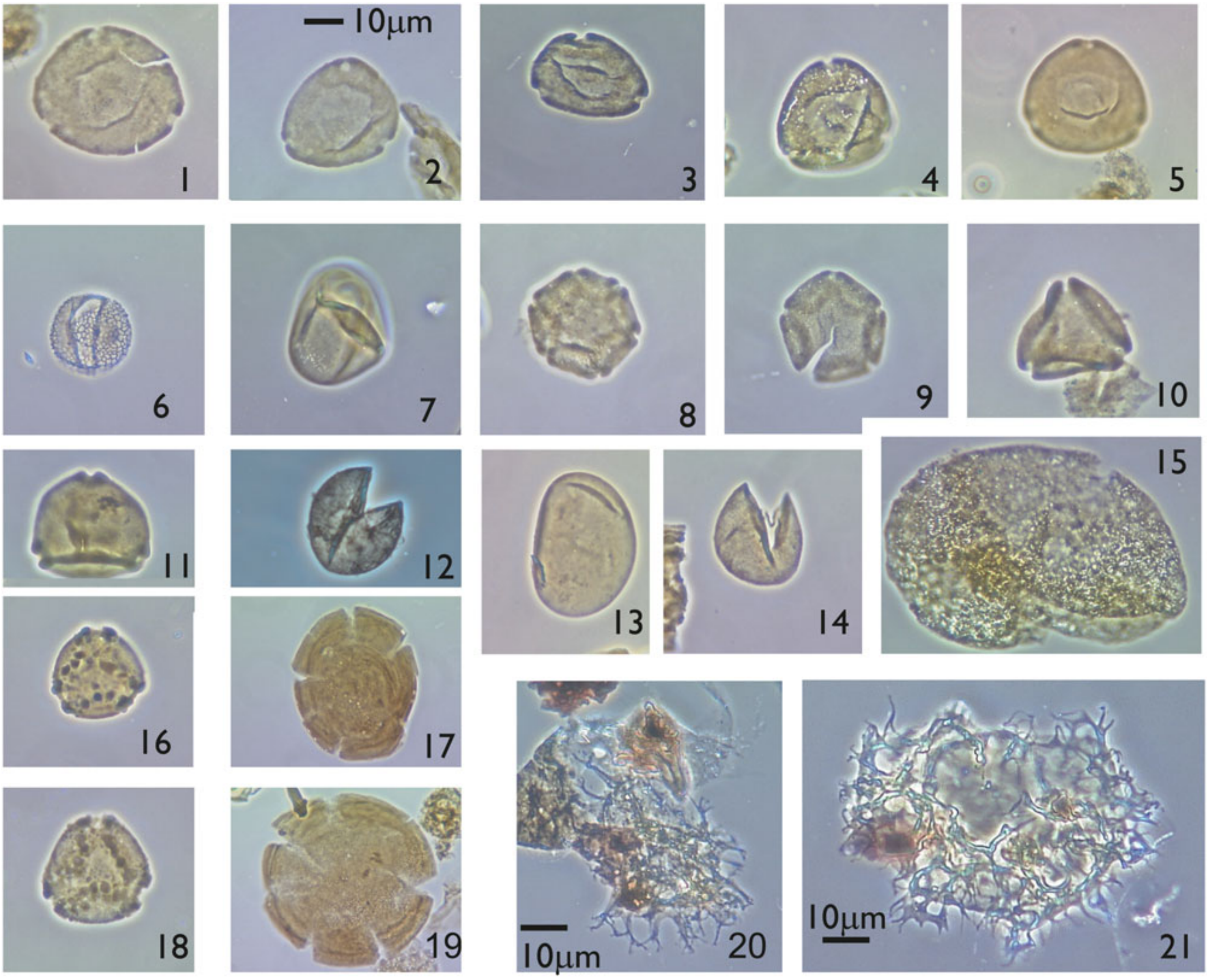


**Figure 5** Palynomophs from the Prestfjall Formation on Suðuroy, 1–19 at the same scale.1, 2 *Caryapollenites circulus*, Rokhagi mine, Sample M8 slide 1, England finder reference W38/2 and Sample M10, England finder reference V42. 3 *Momipites anellus* Rokhagi mine Sample M8, England finder reference U39. 4 *Momipites tenuipolus,* Rokhagi mine sample M8, T47/4. 5 *Caryapollenites veripites* Rokhagi mine sample M10, England finder reference X36/1. 6 *Arecipites* sp. KOLBHI-04, 219.14 m, England finder reference R26/4. 7 *Deltoidospora diaphana*, Rokhagi mine sample M8, England finder reference U42/4. 8,9, *Alnipollenites verus* Rokhagi mine sample M2, England finder references X43/3 and S40/4. 10 *Alnipollenites trina,* Rokhagi mine sample M2, England finder reference O28. 11 *Triatriopollenites subtriangulus* Rokhagi mine sample M4, England finder reference U41. 12 *Inaperturopollenites hiatus* KOLBHI-04, 214.0 m England finder reference V43/2. 13, *Laevigatosporites haardtii* Rokhagi mine sample M4, England finder reference S32. 14 *Inaperturopollenites distichiforme* Rokhagi mine sample M4, England finder reference S43. 15 *Pityosporites labdacus* Rokhagi mine sample M8, England finder reference T37/2. 16, 18, *Phaseoidites stanleyi* Rokhagi mine sample M2, England finder references M44 and T44/2. 17, 19, *Polycolpites* sp. (Rubiaceae) Rokhagi mine sample M8, England finder references T44/2 and S39/4. 20, *Spiniferites ramosus* subsp. *ramosus* KOLBHI-04, 217.83 m, England finder reference M37/1. 21, *Areoligera* cf. *coronata* KOLBHI-04 217.35 m, England finder reference J26/1. Figured material is stored in the museum collection of the University of Aberdeen.

2004). These show repeated depletion trends (Fig. 6), indicative of fluctuation in substrate stability and biomass in the catchment. Mobile element depleted samples correspond to more diverse, mid-seral succession palynofloras (Vitousek 2004; Jolley *et al.* 2008). These were derived from moderately stable substrates within the catchment at periods of lower lake water levels. Low weathering ratios are positively correlated with low diversity, high dominance palynofloras, and are characteristic of deeper lake states (Fig. 6).

Using an approach similar to that of Vitousek (2004), Sheldon (2003) and Sheldon & Tabor (2009), residual magnesium oxide (MgO) concentrations were calculated for the sedimentary rocks sampled. In the uppermost part of the KOLBH1-04 cored succession, concentrations of MgO rise in relation to the average value for Beinisvørð Formation basalts (Fig. 6). This rise is partly due to the occurrence of a volcaniclastic sandstone at 219.4 m, but increasing values from 217.0 m, continuing up section imply increasing volcanic input in the uppermost Prestfjall Formation.

## 3. Thickness variation of the Prestfjall and Hvannhagi formations on Suðuroy

### 3.1. Prestfjall Formation

Observations on the thickness and facies of the Prestfjall Formation on Suðuroy are largely dependent on limited exposures (e.g., Fig. 2) and the measurements of Rasmussen & Noe-Nygaard (1970; Supplementary Data S3). Many of their measured sections (see Fig. 7a) were established in now long-closed coal mine adits and coal prospecting excavations. Additional data from the KOLBH1-04 borehole, field observations, and from the photographic profile of the west Suðuroy cliff line are included here (Passey *et al.* 2016). With these additional data, the creation of isopach maps and integration of palynological data, a modified depositional environment model can be proposed.

An isopach map for the gross thickness of the Prestfjall Formation on Suðuroy (Fig. 7a), shows the thickest deposits to be centred on the west side of the Rokhagi valley, in the north and

https://doi.org/10.1017/S1755691022000056 Published online by Cambridge University Press

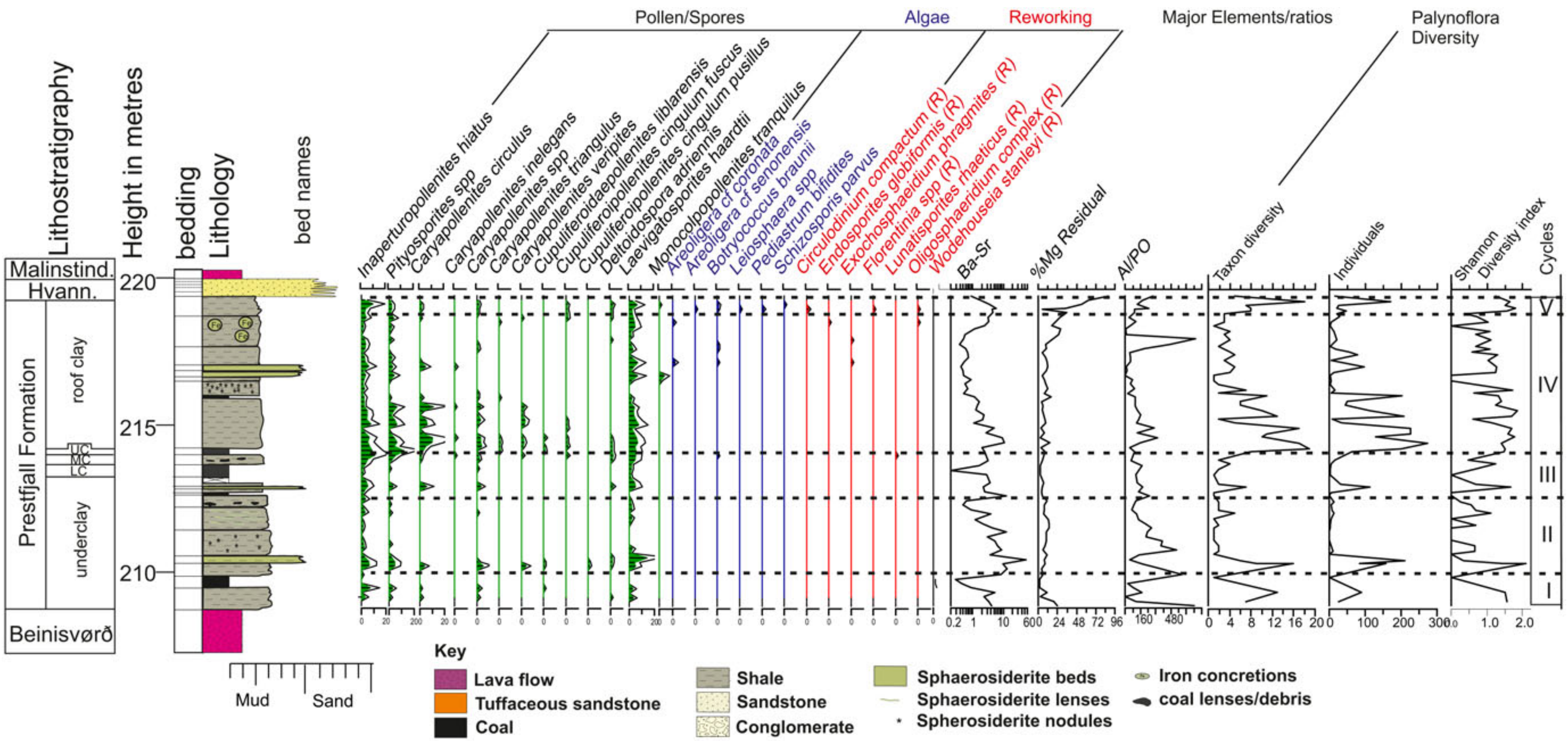


**Figure 6** KOLBH1-04 borehole lithostratigraphy, lithology log and selected palynology data expressed as square roots. Lithology abbreviations: LC = 'lower coal'; MC = 'mid clay'; UC = 'upper coal'; Hvann. = Hvannhagi Formation. Plots for weathering indexes are derived from flame atomic absorption photospectrometry analysis (ratios Ba:Sr and Al:P) highlight cyclicity in the Prestfjall lacustrine depositional system. This is also reflected in the palynofloral diversity plots which show high diversities in intervals of more mature sediment deposition in the catchment. The thin sequence V interval is marked by the occurrence of dinoflagellate cysts and reworked palynomorphs. This is interpreted as a tidally influenced fluvial channel deposit, the rise in relative sea level initiating an integrated drainage system. This upper Prestfjall Formation incursion event is correlative with a similar event seen in the Gasadalur-1989 borehole. Taxon diversity =number of species in a sample, Individuals = number of specimens in standardised slide mount. Together with the Shannon diversity index of the palynoflora, these are used to define depositional cycles (I–V). Percentage of magnesium residual is calculated by expressing the % value of magnesium oxide (MgO) in the Prestfjall Formation samples against the average MgO value for late Beinisvørð Formation.

https://doi.org/10.1017/S1755691022000056 Published online by Cambridge University Press

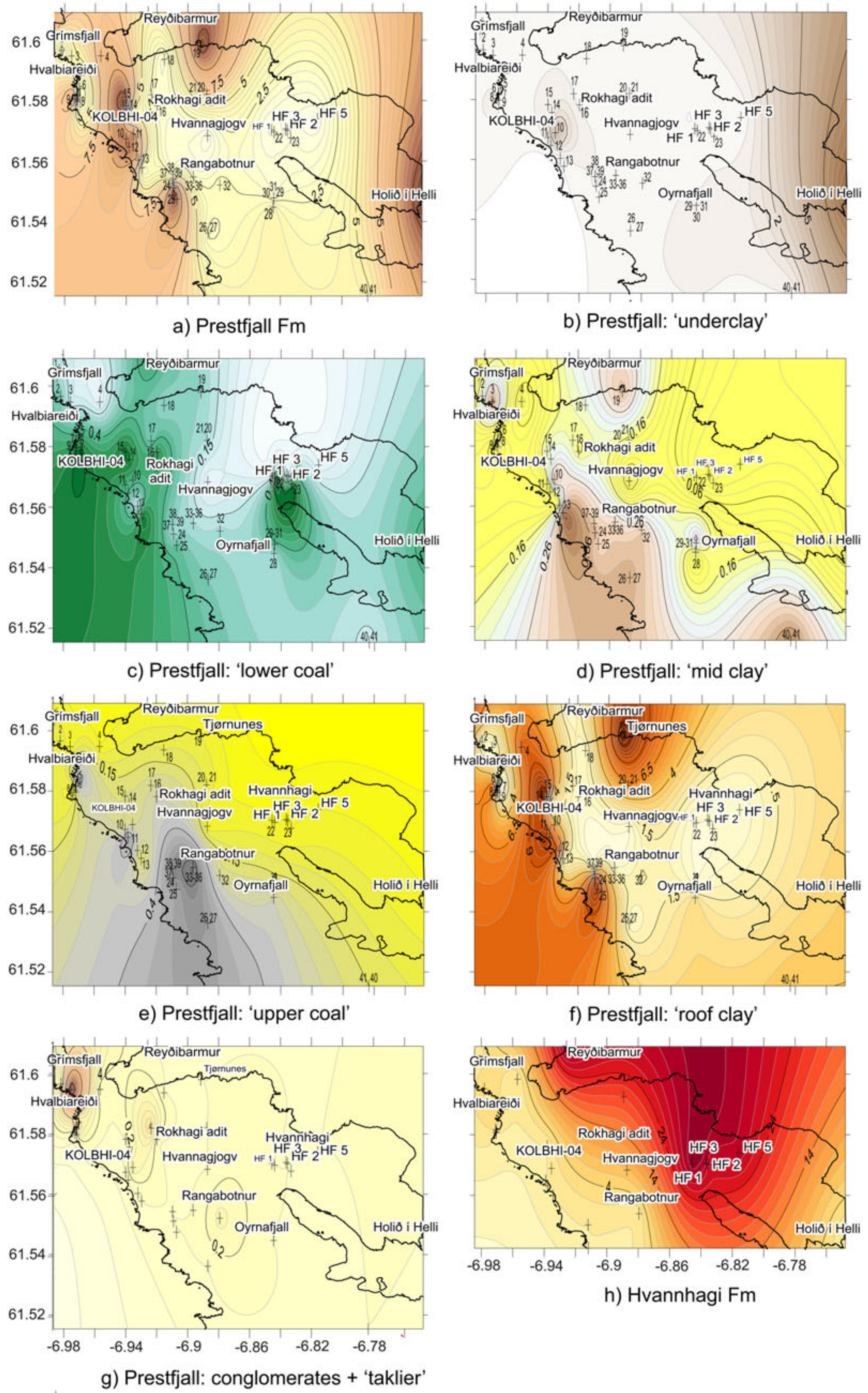


**Figure 7** Isopach maps for the Prestfjall Formation and named bed units on Suðuroy. Data presented here indicate that these beds are to varied extent, diachronous facies within the Prestfjall Formation. These maps were constructed from the profile data presented in Rasmussen & Noe Nygaard (1970), supplemented by data from the boreholes and sections discussed here. These locations are shown using the profile numbers of Rasmussen & Noe Nygaard (1970). Isopach maps are contoured in metres, and differential shading is used to highlight the contours with the most intense shading used for the thickest strata. Shading colour is changed to emphasise different lithologies. The data are presented at Supplementary Data S3.

in the extreme east at Holið í Helli [61.547N, 6.746W]. Overall, the Prestfjall Formation thins abruptly across the centre and northeast of the island centred around Stapin ([61.583N, 6.829W] Figs 1, 7a). There is no evidence for the Prestfjall Formation having been deposited *in situ* in the Stapin area, although allochthonous rafts of Prestfjall Formation occur in thick sills

https://doi.org/10.1017/S1755691022000056 Published online by Cambridge University Press

intruding the Hvannhagi Formation (Fig. 4a). At Stapin, volcaniclastic Hvannhagi Formation conglomerates and shales overlie an older, Beinisvørð Formation volcanic vent (the 'Stapin Vent'; Passey 2004; Passey & Jolley 2009). Northwest of Stapin, thick Prestfjall Formation coals and shale beds are inferred from peperitised rocks in the base of the Hvannhagi Formation succession at Reyðibarmur ([61.610N, 6.924W] Figs 1, 7a). These exposures are dissimilar to others of the Prestfjall Formation in being overlain by a thick volcaniclastic Hvannhagi Formation succession (Fig. 7h).

Thin profiles of the Prestfjall Formation have been recorded over central Suðuroy, extending from Tjørnunes [61.598N, 6.890W] on the northeast coast to Fámjin [61.525N, 6.881W] on the central west coast. Although exposures are limited, a profile comprising basaltic lava flows and thin volcaniclastic sediments at Hvannagjógv [61.569N, 6.889W] indicates that a localised flow terrain may have influenced part of the western limit of the Prestfjall Formation lacustrine basin. Difficulties in differentiating intrusive from extrusive basalt units also appear to have resulted in profile 20 near Tjørnunes being underestimated or misinterpreted (Fig. 7a; Rasmussen & Noe-Nygaard 1970). These central Suðuroy extrusive volcanics and the intrusion of sills into the Prestfjall Formation are orientated from Reyðibarmur in the north, south southeast to profiles 29, 30 and 31 on Oyrnafjall ([61.547N, 6.849W] Fig. 7a, d, e, f; Rasmussen & Noe-Nygaard 1970). Here, basalt intrusions invade the Prestfjall Formation in a manner similar to that at Reyðibarmur. Deposition within the southern area of the lacustrine basin was thickest at Rangabotnur [61.551N, 6.890W] and to the west (Fig. 7a), while east of profile 36, pre-existing topography resulted in a thin sedimentary succession.

Isopach mapping of the gross thickness of coaly sediments of the Prestfjall Formation was undertaken by Ellis *et al.* (2009). In addition to mapping the gross thickness, isopach mapping of the five informal units of the Prestfjall Formation (Rasmussen & Noe-Nygaard 1970) has highlighted incompatibilities between individual profiles, particularly with reference to the KOLBH1-04 borehole. Isopach mapping of the 'underclay' (Fig. 7b) shows that the borehole contains an anomalously thick unit in comparison to those only a few tens of metres away (e.g., Figs 4, 6). In contrast, the 'lower coal' (Fig. 6) is significantly thinner in the KOLBH1-04 borehole and in profiles 10–13 (Fig. 7c) immediately to the south, than in the Rokhagi profile (Fig. 4). The regular occurrence of coal lenses and flasers in the 'underclay' of KOLBH1-04 and profiles 10–13 indicate lateral facies change from these lacustrine proximal shales to lacustrine distal, durain-rich coals. Comparison of palynological data from the Rokhagi mine profile with that in the KOLBH1-04 borehole (Figs 4, 6) supports this interpretation of the lithological data. Based on palynological data, both the 'upper' and 'lower' coals in the KOLBH1-04 profile are age equivalent to the 'upper coal' in the Rokhagi mine profile. Similarly, the 'lower' coal of the Rokhagi mine profile is correlative with the 'underclay' of the KOLBH1-04 borehole.

Given that the carbonaceous content of the Prestfjall Formation is allochthonous, lateral variation in the concentration of drifted organic debris would have resulted from water current and wind effect on the lake basin. Prevailing wind directions from the northwest in the Selandian to lower Ypresian are indicated from tephra distribution in the North Sea and Faroe–Shetland basins (Knox & Morton 1988). Amplified by fluvial input down the regional slope from the north northwest, this would have resulted in accumulations of woody debris along the distal, eastern margin of the lacustrine basin, against the Reyðibarmur–Hvannagjógv–Oyrnafjall zone (Fig. 7c). Although the highly carbonaceous profiles recorded in mines on the east side of the Rokhagi valley are not the thickest of the Prestfjall Formation successions (Fig. 7a, c), the thicker coal units in these locations would have been subjected to greater compaction (compaction factors of 6–10; Elliott, 1984) than areas of dominantly clastic sedimentary rocks (compaction factors of 1.2–2.0; Mondol *et al.* 2007; Bjørlykke *et al.* 2009). Decompaction of these profiles suggests that the eastern margin of the Prestfjall Formation basin was at its deepest on the eastern side of Rokhagi.

Conglomerates and normally graded pebbly sandstones recorded at the top of the Prestfjall Formation in the northwest of the basin (Rasmussen & Noe-Nygaard 1970) mark a period of uplift and erosion. These deposits have also been recorded on the west coast of Suðuroy near Grímsfjall ([61.598N, 6.987W] Fig. 2d). Here, a paleovalley (15–20 m in depth) eroded into the Prestfjall Formation was filled by pillow-based, columnar jointed lava flows of the Malinstindur Formation. The erosive, conglomerate and sandstone filled fluvial channels present in the northwest of the lacustrine basin are not observed to cut the red-brown claystones of the 'takleir' unit of the 'roof clay'. Combination of conglomerate–sandstone filled channel thicknesses with those of the 'taklier' claystone (Fig. 7g) indicate that the claystones were overbank facies of the fluvial channel fill sandstones and conglomerates. This combined 'taklier' and conglomerate unit is confined to the northwest of the Prestfjall Formation lacustrine basin (Fig. 7g), coincident with the lava filled valley eroded into the top of the Prestfjall Formation at Grímsfjall (Fig. 2d). Together, these indicate incision of a limited fluvial drainage system into the carbonaceous Prestfjall Formation. Uplift and incision of this area could have been a response to localised thermal uplift of the area following the onset of Malinstindur Formation volcanism. However, this erosion occurred in the same period as uplift and incision of the eastern margin of the Faroe–Shetland Basin following relative sea level fall. Here, basin flank uplift resulted in the rejuvenation of shelf margin drainage systems to form the age equivalent Flett Unconformity (Shaw Champion *et al.* 2008; Hartley *et al.* 2011; Jolley *et al.* 2021).

## 3.2. Hvannhagi Formation

The gross thickness isopach for the Hvannhagi Formation (Fig. 7h) clearly identifies a depocentre in the northeast of Suðuroy. Composed of >25 m thickness of tuffs and volcaniclastic sedimentary rocks (Passey & Jolley 2009), these are at the thickest between Stapin and Hvannhagi proximal to the source. These rocks thin significantly to the south with distance from source, where ~3 m of tuffaceous rocks are recorded at Holið í Helli (Fig. 3). Mapping the western limit of these rocks is problematic, their exposure being obscured by thick dolerite sills. However, they appear to pass laterally into volcaniclastic sedimentary rocks and basaltic lava flows at Hvannagjógv. Overlying the intruded, fluidal peperitised Prestfjall Formation strata exposed at Reyðibarmur, the Hvannhagi Formation includes normally graded volcaniclastic sandstones, lapillistones, and tuffs. These are composed of palagonitised volcanic glass, larger fragments exhibiting cuspate edges. The absence of intrusions in these sedimentary rocks suggests that the peperitisation of the underlying Prestfjall Formation took place during shallow burial, prior to Hvannhagi Formation deposition.

Approximately 2 m above the base of the Hvannhagi Formation at Leirbakki ([61.581N, 6.831W] Fig. 1), clast supported conglomerates made up of 2 cm–8 cm pebbles occur in lensoid bodies up to 10 m across (Fig. 2a, c). Resting unconformably on the surface of the late Beinisvørð Formation Stapin Vent, the conglomerates include large blocks up to 50 cm wide, but are overlain by up to 1 m of finely bedded mudstones which include some thin, bright coals up to 2 cm thick (Fig. 2a).

https://doi.org/10.1017/S1755691022000056 Published online by Cambridge University Press

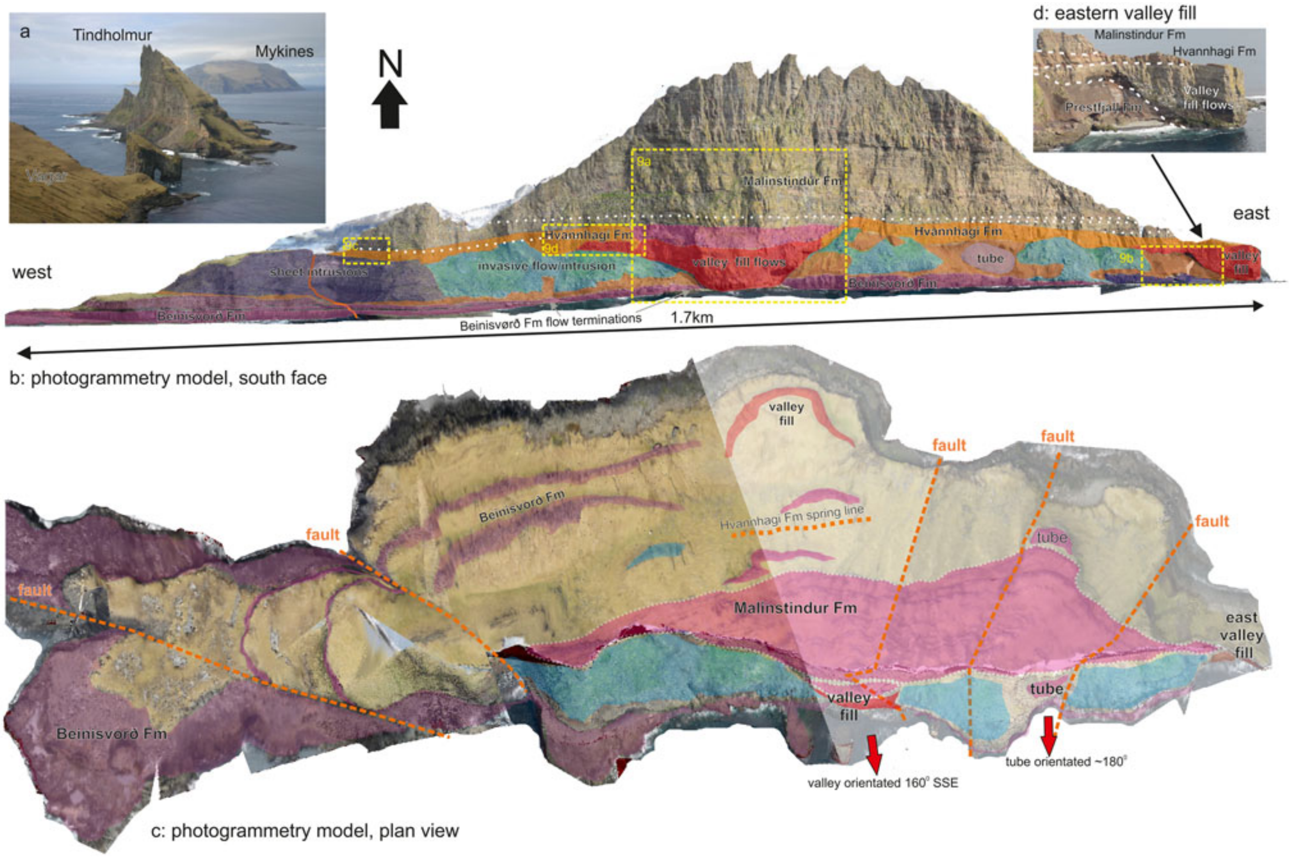


**Figure 8** Tindhólmur interpreted photogrammetry model. Figure 8a, view of Tindhólmur northwest from Vágar, with Mykines in the distance. The south face of Tindhólmur is shown in interpreted model Fig. 8b. Transparent shading is used to clarify geological relationships; Beinisvørð Formation, purple; invasive flows and sills, blue; Prestfjall Formation, red; Hvannhagi Formation, orange; Malinstindur Formation valley fill flows, red; and Malinstindur Formation, pale purple. Formation boundaries are picked out by white dashed lines, other intra formation boundaries by white dotted lines. F = fault, yellow dashed boxes define position of other figures. 8c plan view of Tindhólmur showing poor rock exposure on the northern face, although the Hvannhagi Formation forms a distinct spring line where it intersects the surface. Valley fill flows can be seen to extend to the north in the centre of the island, as does the lava tube exposed on the east of the island. The faults evident from the model show little vertical movement and are assumed to be predominantly strike-slip. Yellow dashed boxes show position of photographs in Fig. 9.

These shales and drifted coals yielded a lacustrine palynoflora dominated by taxa common in transported assemblages (*Inaperturopollenites hiatus* and *Pityosporites* spp.). Occurrences of *Caryapollenites circulus* and *Cupuliferoipollenites cingulum subsp. oviformis* in these shales indicate coeval deposition of lowermost Hvannhagi Formation volcaniclastic and upper Prestfjall Formation carbonaceous beds.

A second, different flora was recorded from the upper part of the Hvannhagi Formation succession in the Svalbaá stream [61.571N, 6.835W], near Trongisvágur (Fig. 1). Here, *C. circulus* occurs commonly with *Caryapollenites inelegans* and *Caryapollenites veripites* in a coal rip-up clast within the upper conglomerate beds. This clast along with others in the uppermost Hvannhagi Formation are clearly derived from the Prestfjall Formation coals, presumably from an area in the northwest where they have been largely eroded away.

## 4. Pre-rift to syn-rift rock succession on Vágar and adjacent islands

The northern exposure of the Prestfjall and Hvannhagi formations crops out on the islands of Tindhólmur and Vágar (Fig. 1). Exposure is largely restricted to coastal cliffs, which are mostly inaccessible, other than when viewed from out to sea. Because of this inaccessibility combined with poor exposure, there are no detailed published records of the Beinisvørð–Malinstindur transition in this area. A borehole (Gásadalur 1989-1) drilled near Bøur on Vágar penetrated this succession and this provides the most comprehensive record of Prestfjall and Hvannhagi formations sedimentary facies on Vágar. The small island of Tindhólmur presents the least disrupted exposure of the Beinisvørð–Malinstindur transition and is considered first.

### 4.1. Tindhólmur

The south facing cliffs of the island of Tindhólmur expose a section through the Prestfjall and Hvannhagi formations and the base of the Malinstindur Formation (Fig. 8). On Mykineshólmur (Fig. 1) and the on western end of Tindhólmur, thick Beinisvørð Formation simple lava flows dip to the southeast. On Tindhólmur, these are overlain by the Prestfjall Formation which is composed of horizontally bedded volcaniclastic coarse-grained to fine-grained sandstones in beds 10 cm–30 cm thick. These sandstones are ~5 m thick in the west, thickening abruptly over a Beinisvørð Formation lava flow termination to ~28 m over the centre and east of the island. There is no evidence of a significant erosive unconformity at the base of the Prestfjall Formation, the sedimentary rocks having been deposited at the eastern side of a series of Beinisvørð Formation simple lava flow terminations (Fig. 8).

Numerous shallow invasive flows and sills are exposed at the boundary between the Prestfjall Formation and the overlying Hvannhagi Formation, obscuring the nature of the contact (Fig. 8b). In the centre of the island, a 260 m wide channel eroded into the underlying Prestfjall Formation was filled with crudely bedded lava flows, which overstep the edge of the channel structure onto the upper surface of the Prestfjall Formation

https://doi.org/10.1017/S1755691022000056 Published online by Cambridge University Press

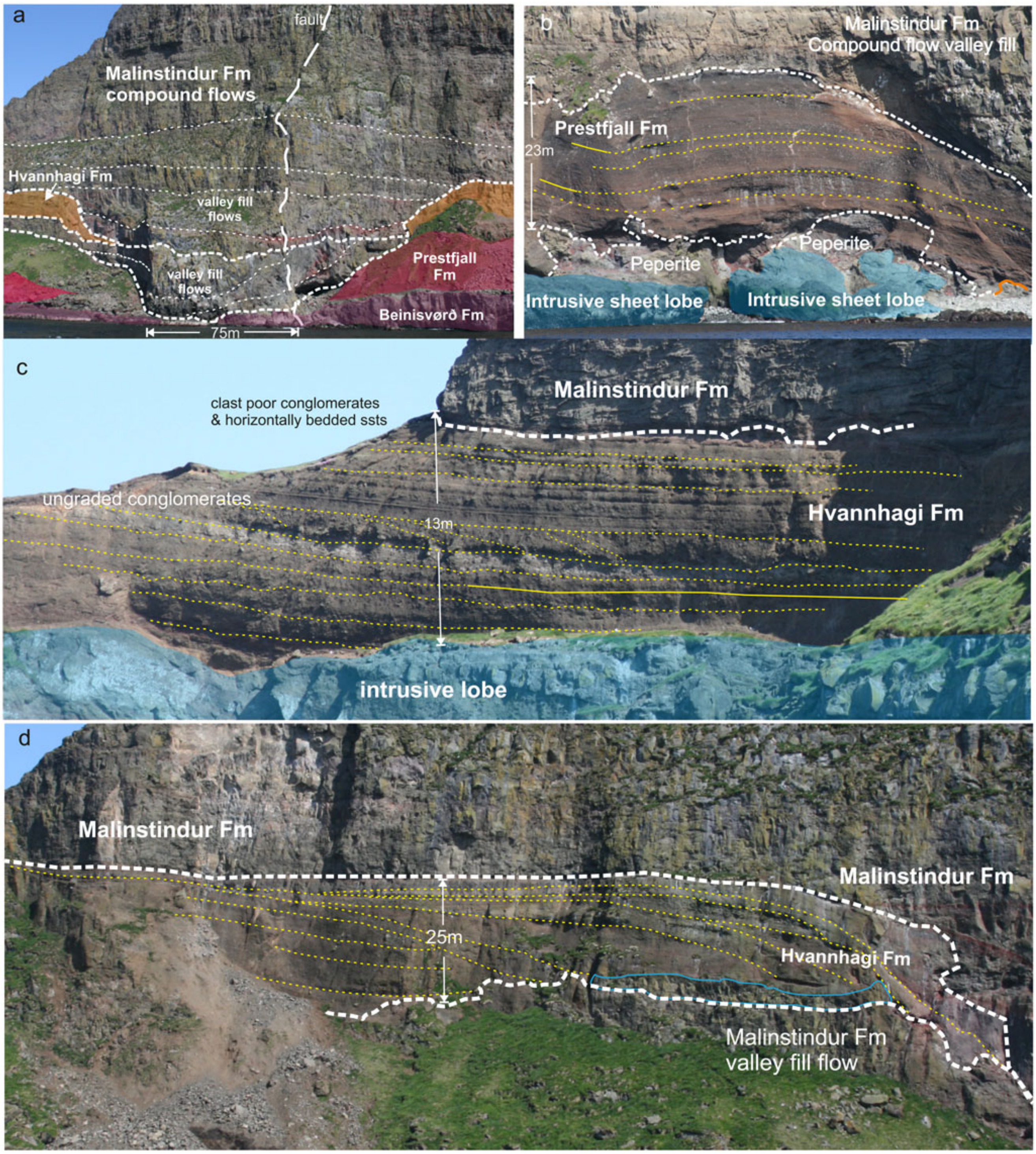


**Figure 9** Interpreted field photographs of Tindhólmur taken from sea level: (a) central valley fill showing both pre-Hvannhagi Formation and post-Hvannhagi Formation valley fill Malinstindur Formation lava flows. The oldest set of valley fill flows pre-date the Hvannhagi Formation, which can be seen to overlie them at the margins. Later valley fill flows were emplaced into a shallow valley eroded into the Hvannhagi Formation as part of the overlying Malinstindur Formation succession. (b) Parallel bedded Prestfjall Formation volcaniclastic sandstones incised by the eastern valley, showing Malinstindur Formation compound flow fill; (c) Hvannhagi Formation exposure at the western end of island showing transition from hyperconcentrated flow deposits to matrix supported and cross-bedded conglomerates and sandstones deposited under fluvial flow; and (d) Hvannhagi Formation on the western flank of the central valley fill succession.

(Figs 8, 9a). Orientated 160° south southest, this channel occurs in the middle of the south face of Tindhólmur, its eastern margin being influenced by a north northeast–south southwest trending fault (Figs 8, 9, 10), interpreted as dominantly strike slip with some minor downthrow component to the west. The upper surface of these valley fill compound lava flows is reddened to a few centimetres (Fig. 9a), resulting from an eruptive hiatus and weathering of the lava flow surface.

A second steep sided valley fill is partly exposed at the eastern tip of the island (Figs 8b and 9b). The valley is >150 m wide, the eastern margin having been eroded away. The valley was incised through Prestfjall Formation sandstones, and was subsequently filled by compound lava flows of the Malinstindur Formation (Figs 8b, d, 9b). Overlying the valley fill of compound flows is a 4.8 m thick succession of mostly clast supported, coarse polymictic basalt clast conglomerates of the Hvannhagi Formation

https://doi.org/10.1017/S1755691022000056 Published online by Cambridge University Press

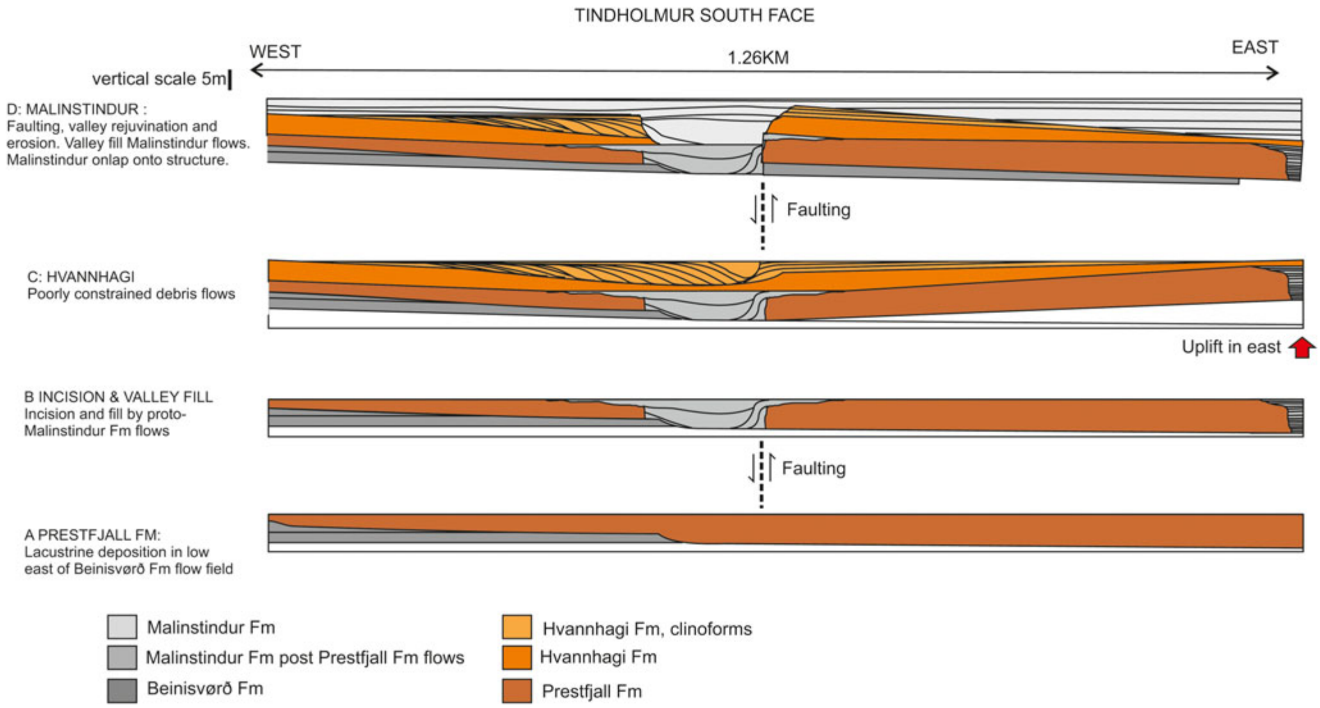


**Figure 10** Schematic Tindhólmur depositional history diagram. The fault on the eastern margin of the central valley is assumed to have been dominantly strike-slip. However, it also focussed erosion, developing accommodation space for subsequent valley fill lava emplacement.

(Fig. 8b). These thicken into the centre of Tindhólmur, reaching 24 m–26 m thickness on either side of the central valley, thinning to 7.2 m in the west (Fig. 8b). In this unit, low angle, trough cross bedding is evident across the island, with evidence of incision and erosion of earlier Hvannhagi Formation sediments. A well-exposed section (Fig. 9c) in the west of the island shows that the upper Hvannhagi Formation transitioned upsection from the clast supported conglomerates to clast poor conglomerates and volcaniclastic sandstones, some with cross bedding.

The Hvannhagi Formation is interpreted to have been deposited as a volcanic lahar (Smith & Lowe 1991). Clast rich, ungraded beds were deposited under hyperconcentrated flow. Clast poor, weakly horizontally bedded and cross bedded sandstones in the upper beds (Fig. 9c) reflect the transition from deposition by hyperconcentrated flow to streamflow. Shallow incisions of younger, clast rich conglomerate beds into older Hvannhagi Formation conglomerates are associated with wide channels and clinoforms, suggesting that these were deposited by a dilute lahar flow (*cf.* Pierson *et al.* 2011).

A subsequent period of erosion removed some of the previous valley fill flows and created accommodation space along the axis of the central valley (Figs 9a, 10). Rejuvenation of the Tindhólmur central valley and differential uplift of the east flank by 8 m with respect to the west flank, was calibrated from the photogrammetry model (Figs 8, 9a). Differential movement of one valley flank with respect to the other is attributed to further movement on the valley edge fault (Fig. 10). This irregular topography was onlapped and overstepped by the prograding Malinstindur Formation compound flow field (Figs 8, 9, 10). In addition to infilling the central valley structure, these flows covered the western flank of the central valley before the uplifted eastern flank was submerged (Fig. 10).

## 4.2. Vágar

The Gásadalur 1989-1 borehole (Fig. 1; [62.09471N, 7.40663W]) was drilled on the island of Vágar in 1989, approximately halfway between the villages of Gásadalur and Bøur, penetrating the Malinstindur, Hvannhagi and Prestfjall formations before terminating in the uppermost lava flows of the Beinisvørð Formation. The Prestfjall Formation rests on a basalt lava flow where a sandy paleosol developed (Fig. 11). Overlying this are approximately 11 m of volcaniclastic sandstones and conglomerates attributed to the Prestfjall Formation. These are, in turn, overlain by matrix supported, very poorly sorted, polymictic, granulite to pebble grade volcaniclastic conglomerates of the Hvannhagi Formation. Low-angle cross bedding occurs in the sandstone units of the Prestfjall Formation while the conglomerates of the Hvannhagi Formation appear as unstructured or normally graded beds.

Fifty-two samples from the borehole were analysed for palynology, although recovery was concentrated within the Prestfjall Formation. These palynofloras are similar in composition to those recorded in the Prestfjall Formation of the KOLBH1-04 borehole. Dominated by *Pityosporites* spp. and *Inaperturopollenites hiatus* (Figs 5, 11) these floras are typical of fluvially transported assemblages (Daly *et al.* 2011a). In comparison to Prestfjall Formation records from Suðuroy, *Caryapollenites* species, typical of transitional swamp floodplain communities, occur at lower frequency in the Gásadalur borehole. Palynofloras also decline in diversity and frequency in the upper beds of the Prestfjall Formation. Common *Laevigatosporites haardtii and Deltoidospora adriennis* fern spores were recorded in the upper beds of the Prestfjall Formation (Fig. 11). *Laevigatosporites haardtii* is derived from ferns which exploited disturbed substrates and newly exposed overbank areas (Collinson 2002; Jolley *et al.* 2009), while the parent plant of *D. adriennis* was associated with colonisation of crevasse splays and inter channel sand and mud banks (Jolley *et al.* 2009; Daly *et al.* 2011a). These beds also yielded common *Triporopollenites coryloides* (Myricaceae, Myrtle types) which indicate dryer, better-drained substrates associated with sandy floodplains or sandy channel margins.

In addition to these indications of a dynamic depositional environment, the dinocyst *Impletosphaeridium ligospinosum*, the prasinophycean algae *Leiosphaeridia* spp., and reworked Mesozoic palynomorphs occurred in the uppermost siltstones of the Prestfjall Formation (40.29 m–40.20 m; Fig. 11). Characteristic of low salinity marginal marine conditions, their occurrence indicates that the upper Prestfjall Formation at Gásadalur

https://doi.org/10.1017/S1755691022000056 Published online by Cambridge University Press

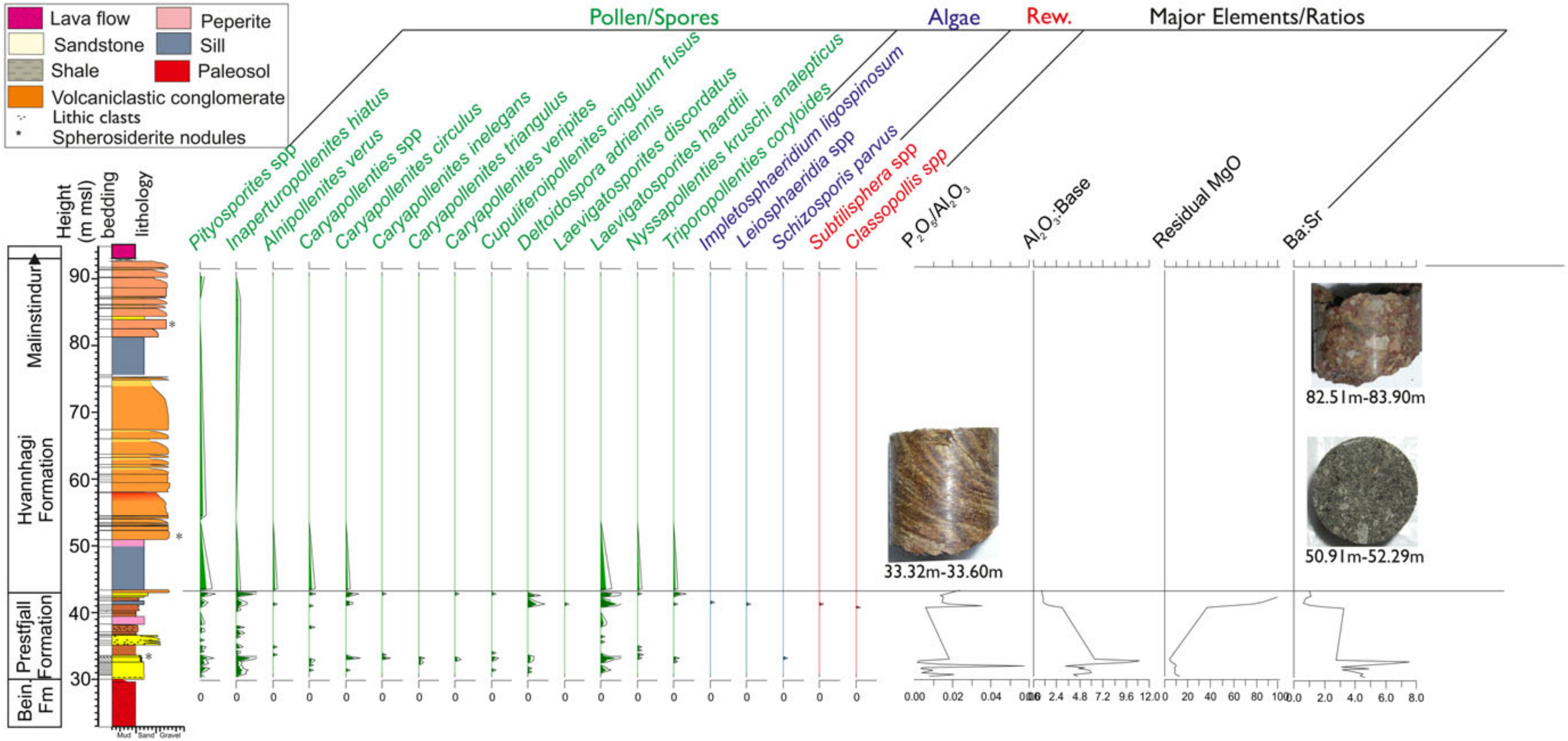


**Figure 11** Gásadalur 1989-1 borehole lithostratigraphy, lithology log, and selected palynology data expressed as square roots. Plots for weathering indexes are derived from X-ray fluorescence analysis (major and trace element ratios $Al_2O_4$:base, Ba:Sr and $P_2O_4$:$Al_2O_4$) The photographs of pieces of the 5 cm core show cross bedded sandstones of the Prestfjall Formation (33.32 m–33.60 m) and two cores of the immature, clast supported conglomerates of the Hvannhagi Formation.

https://doi.org/10.1017/S1755691022000056 Published online by Cambridge University Press

was deposited within tidally influenced fluvial channels. As with the uppermost bed of the Prestfjall Formation in the KOLBH1-04 borehole on Suðuroy, the presence of reworked Mesozoic palynomorphs (Fig. 11), indicates a drainage system integrated outside the lava field. The source area of these reworked palynomorphs is currently unknown, as with other occurrences of Mesozoic and some Carboniferous taxa in the upper Malinstindur Formation and Sneis Formation interbeds (Passey & Jolley 2009). Given the transition into a marine environment in the Faroe–Shetland Basin to the southeast (Jolley *et al.* 2021), a clastic source to the northwest is thought probable.

The pollen and spore record from the Prestfjall Formation in the Gásadalur borehole was derived from disturbed fluvial margin and flow top habitats, deposited in a fluvial environment. Because the overlying Hvannhagi Formation was deposited by a high-energy system derived from an active volcanic zone, the palynofloras are poor. Only low frequencies of fluvially transported taxa occur. However, they do indicate that the catchment area of the Hvannhagi Formation conglomerates was vegetated to some extent.

Samples used for palynological analysis were also subjected to XRF analysis of major and trace elements (Fig. 11, Supplementary data S2). The plot of MgO values against an average value for the Malinstindur Formation highlights the first evidence of volcanism in the uppermost few centimetres of the Prestfjall Formation prior to the comprehensive volcanism of the Malinstindur Formation. This is supported by the Ba:Sr and $Al_2O_4$:base ratios which drop significantly in this interval.

The architecture of the Prestfjall and Hvannhagi formations deposits around Vágar is obscured by the inaccessible nature of the exposures. Boat surveys have proven to be of limited value because of the low-angle of view, although Rasmussen & Noe-Nygaard (1970) recorded complex disruption of the Prestfjall Formation from basaltic intrusions. Because of this lack of accessibility, a photographic survey was undertaken from a helicopter which provided the basis for a photogrammetry model (Passey *et al.* 2016). This model provided coverage of the Prestfjall and Hvannhagi formations over the islands of Tindhólmur and western Vágar.

The succession drilled by the Gásadalur 1989-1 borehole is exposed in inaccessible sea cliffs southeast and northwest of the village of Bøur on Vágar. Creation of a photogrammetry model from the stereo photographic survey of the western coastline of Vágar has allowed these sections to be placed in the wider context of the transition between the Beinisvørð and Malinstindur formations (Fig. 12).

Mapping of the Beinisvørð–Prestfjall Unconformity surface (Passey & Varming 2010) identified an east southeast dip across Vágar. The intra Malinstindur Formation Kvívík Beds (Passey & Jolley 2009), also showed a dip to the east, indicating little overall structural change during the deposition of the Prestfjall and Hvannhagi formations. Examination of photogrammetry profiles of the west coast of Vágar showed that the interval between the Beinisvørð–Prestfjall Unconformity surface and the base of the Malinstindur Formation thins from Bøur [62.086N, 7.369W] in the south to Barðið [62.143N, 7.457W] in the north. From Barðið to Ritunøva [62.145N, 7.341W] on the north coast, the same interval thins to a few metres before it passes below sea level to the west of Viðvík ([62.124N, 7.356W]; Figs 1, 12).

Thinning of the Prestfjall–Hvannhagi formation interval to the north and east of Vágar is linked to the underlying topography at the cessation of Beinisvørð Formation eruptions. In north-western Vágar, the exposed upper Beinisvørð Formation is composed of a thick sequence of compound basalt flows onlapped by a succession of dipping simple lava flows and volcaniclastic rocks, which thicken to the south (Figs 12, 13). These compound lava flows are interpreted to have originated from a low-angle shield volcano point source (Passey & Bell 2007), here termed the Mykines–Vágar low-angle shield volcano. An isopach map for the upper unit of the compound flow field demonstrates a source to the northwest (Fig. 13a). This is honoured by the onlap pattern of the subsequent Beinisvørð Formation simple lava flows, which overlie the compound flow field (Figs 12, 13b). A gravity anomaly, some 15 km north of Mykines was identified by Schrøder (1971); this probably reflects the location of the Mykines–Vágar low-angle shield.

In the cliffs north and south of Gásadalur village, the simple lava flows of the upper Beinisvørð Formation are interbedded with dark red volcaniclastic sandstones and siltstones which thicken to the south (Fig. 12b). Where exposed at Reyðastíggjatangi [62.104N, 7.436W], these are composed of blocky, fissile, red-brown volcaniclastic shales and poorly sorted, fine sandstones ~1.3 m thick. Low angle, trough bedding occurs in exposures of this unit tens of metres to the north. Two of these shale units are exposed, separated by a simple lava flow, the oldest shale resting on south southeast prograding hyaloclastite foresets (Fig. 12a). These hyaloclastites are correlative with a simple lava flow exposed to the north (Fig. 12b). Uppermost Beinisvørð Formation red volcaniclastic sedimentary interbeds persist and thicken to the south southeast towards Bøur before dipping below sea level (Figs 12, 14). Together, the change in volcanic facies and south southeast thickening sandstones reflect an increase in accommodation space south of Gásadalur village. This exploited topography is inherited from the southern margin of the Beinisvørð Formation, Mykines–Vágar low-angle shield volcano. This accommodation space was subsequently filled by the deposition of the Prestfjall and Hvannhagi formations.

Exposure of the Prestfjall Formation on Vágar is limited, cropping out in inaccessible sea cliffs north and south of Gásadalur. A record of 90 cm of shales with coaly material included was made by Rasmussen & Noe-Nygaard (1970) at Hellisgjógv ([62.144N, 7.449W] Fig. 1) in the northwest. No beds of carbonaceous sediment or disseminated woody debris were observed during fieldwork for this study.

Along the coastal cliffs from Gásadalur to Ritunøva, the Prestfjall and Hvannhagi formations are very poorly exposed and were regarded as one unit in the photogrammetry interpretation of the Gásadalur to Bøur section (Fig. 12). From Gásadalur to Bøur, there are isolated clear exposures of the Prestfjall Formation, but as noted by Rasmussen & Noe-Nygaard (1970), the volcaniclastic sedimentary rocks are extensively intruded by sills and invasive lava flows. Near Reyðastíggjatangi (Fig. 14a), a ~18 m thick unit of the Prestfjall Formation crops out. Overlying a basal sandstone bed <2 m thick, red to orange, crudely bedded, poorly sorted, and fine-grained sandstones and mudstones occur. These sedimentary units have a sharp upper contact with the overlying clast-rich conglomerates of the Hvannhagi Formation.

The Hvannhagi Formation in the Gásadalur to Bøur section is thicker and more complex than any recorded previously (Figs 12, 14). Dominantly composed of clast supported, ungraded and normally graded, crudely trough bedded volcaniclastic conglomerates, and thin planar bedded sandstones, these beds are ~4 m thick (Figs 12, 14). Clasts are angular to sub-rounded and composed of basalt derived from flow top and inter flow facies from different lava flows. Examination in the field shows that the matrix of these beds is composed of altered volcanic glass and sand grade volcaniclastic material.

Two depositional phases of the Hvannhagi Formation have been interpreted from the photogrammetry model, but exhibit no obvious lithological difference. The oldest unit occurs along the whole of the Gásadalur to Bøur cliff exposure, except where the latter has been penecontemporaneously eroded (Fig 12, Gásadalur to Bøur section, 14b). In the north, this unit

https://doi.org/10.1017/S1755691022000056 Published online by Cambridge University Press

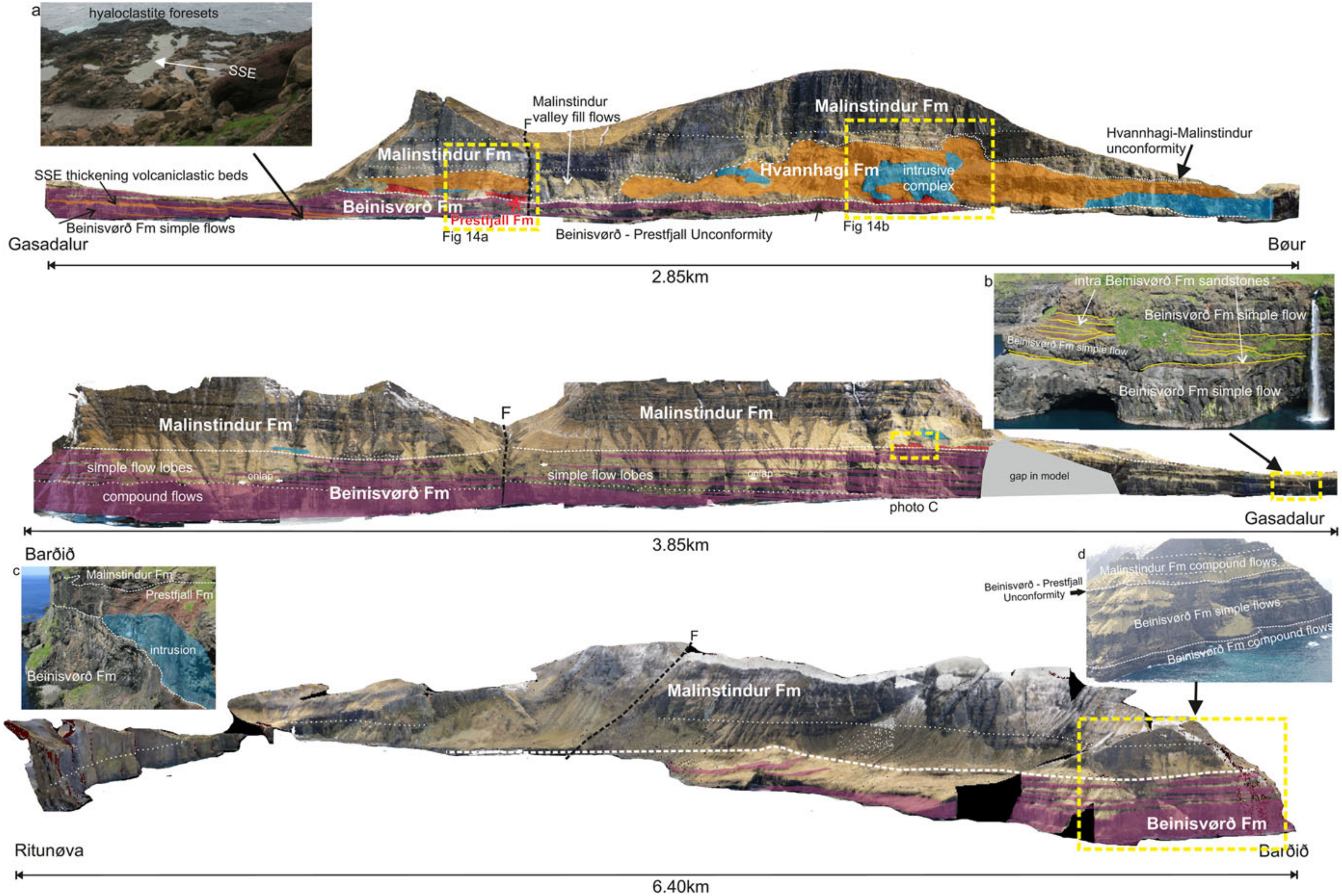


**Figure 12** Interpreted photogrammetry model panels for the coast of Vágar from Bøur to Ritunøva. Transparent shading is used to clarify geological relationships; Beinisvørð Formation, purple; sills, blue; Prestfjall Formation, red; and Hvannhagi Formation, orange. Formation boundaries are picked out by white dashed lines, other intra formation boundaries by white dotted lines. F = fault, yellow dashed boxes define position of other figures in the text. Photograph (a) prograding hyaloclastite foresets towards south southeast on the foreshore at Gasadlaur; (b) intra Beinisvørð Formation volcaniclastic sandstone beds near Gasadalur village; (c) exposure of Prestfjall Formation voclaniclastic sandstones in the cliffs north of Gasadalur. The common habit of sill intrusion into these volcaniclastic sediments is illustrated here; and (d) the coast at Barðið showing compound lava flows overlain by simple flows both of the Beinisvørð Formation. The Beinisvørð–Prestfjall Unconformity is illustrated by the onlap of the Malinstindur Formation compound flows.

https://doi.org/10.1017/S1755691022000056 Published online by Cambridge University Press

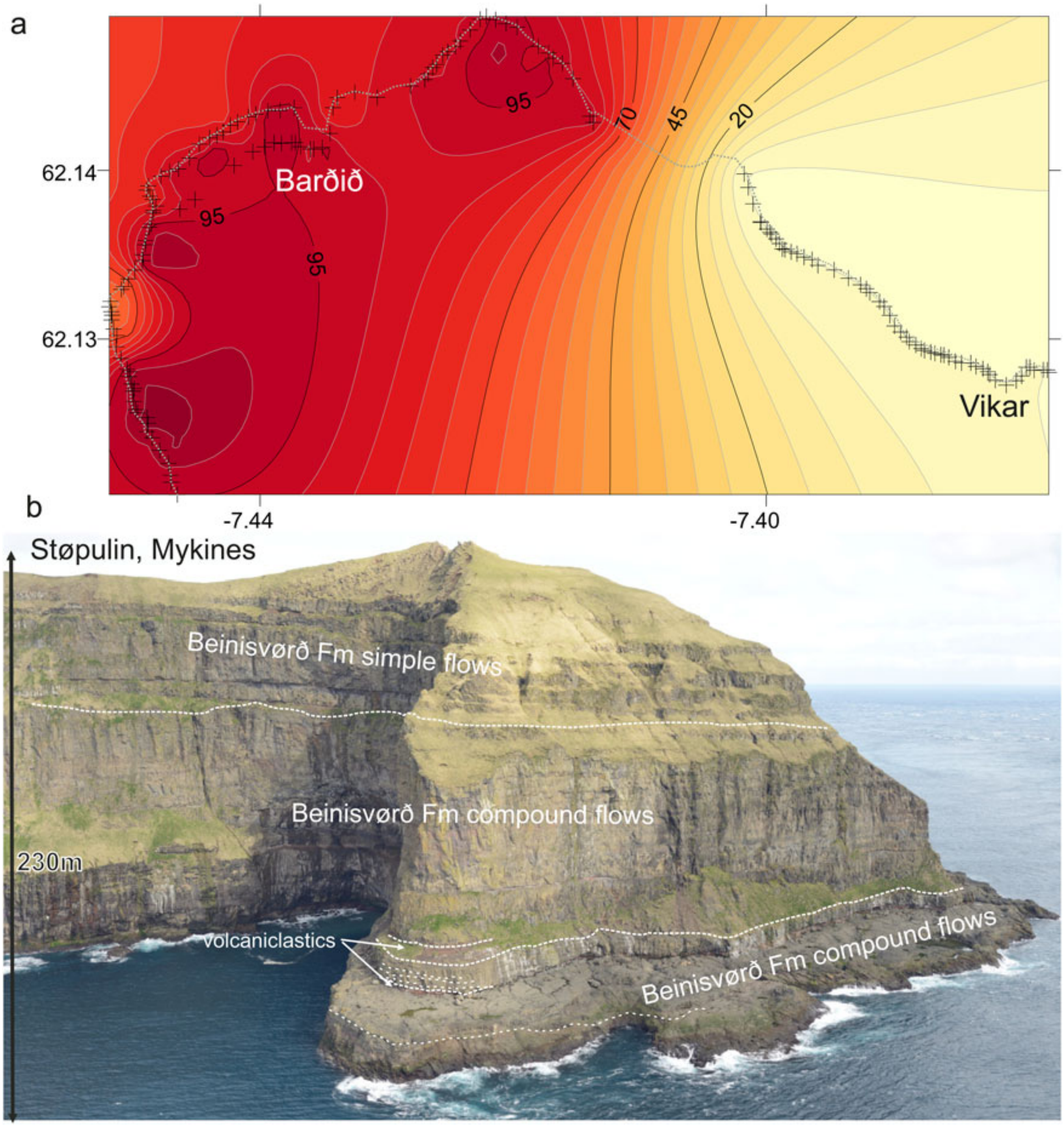


**Figure 13** (a) Isopach map of the upper unit of the compound lava flow succession belonging to the Beinisvørð Formation in north Vágar. This isopach map is contoured in metres, and differential shading is used to highlight the contours with the most intense shading used for the thickest lavas. This map includes the area seen in Fig. 12d; and (b) comparable compound lava flow facies overlain by simple lava flows of the same formation, Støpulin, eastern Mykines (see Fig. 1 for location).

attains 53 m thickness, expanding to ~80 m in the south of the exposure. Overlying this unit is a second, younger conglomerate unit. Separated from the older Hvannhagi Formation conglomerates by shallow invasive flows and sills which follow the boundary, the upper volcaniclastic conglomerates reach a maximum thickness of 94 m (Fig. 14b). The edge of this upper Hvannhagi Formation unit appears to have been penetrated by the Gásadalur 1989-1 borehole. Separated from underlying conglomerates by an intrusive sheet (Fig. 11, 75.6–81.28 m), the upper conglomerate unit (81.28 m–92.62 m) is ~11 m in thickness. However, there is a significant angular unconformity at the boundary between the Hvannhagi Formation and the overlying Malinstindur Formation, with a topographical relief of up to 119 m over 1.2 km of outcrop (Fig. 12 Gásadalur to Bøur section). Due to this unconformity, the depositional architecture of the upper Hvannhagi Formation is difficult to reconstruct.

## 5. Synthesis

Examination of the Beinisvørð–Malinstindur transition exposed on the Faroe Islands has identified a trend in proximal to distal depositional environments from north to south. While all areas were impacted by volcanic activity, those in the Vágar to Tindhólmur area were dominated by lava field processes. Sections exposed on Suðuroy demonstrate dominantly lower energy depositional environments. Accordingly, integration of the depositional environments across these two areas is discussed down the environmental gradient from north to south.

### 5.1. Mykines–Vágar area

Photogrammetry and lava facies evidence of a large compound flow field in northwest Vágar and north Mykines, have confirmed the existence of the Mykines–Vágar low-angle shield volcano. Thick successions of compound lava flows seen on the easternmost tip of Mykines (Fig. 13), indicate that the structure was to the north of Mykines and northwest of Vágar, corresponding to an earlier gravity anomaly interpretation (Schrøder 1971). Subsequently, upper Beinisvørð Formation simple lava flows and volcaniclastic sedimentary rock units onlapped the low-angle shield volcano. These crudely stratified sandstones and shales are lacking in any palynoflora, supporting an origin as weathered and remobilised volcanic ash derived from fissures

https://doi.org/10.1017/S1755691022000056 Published online by Cambridge University Press

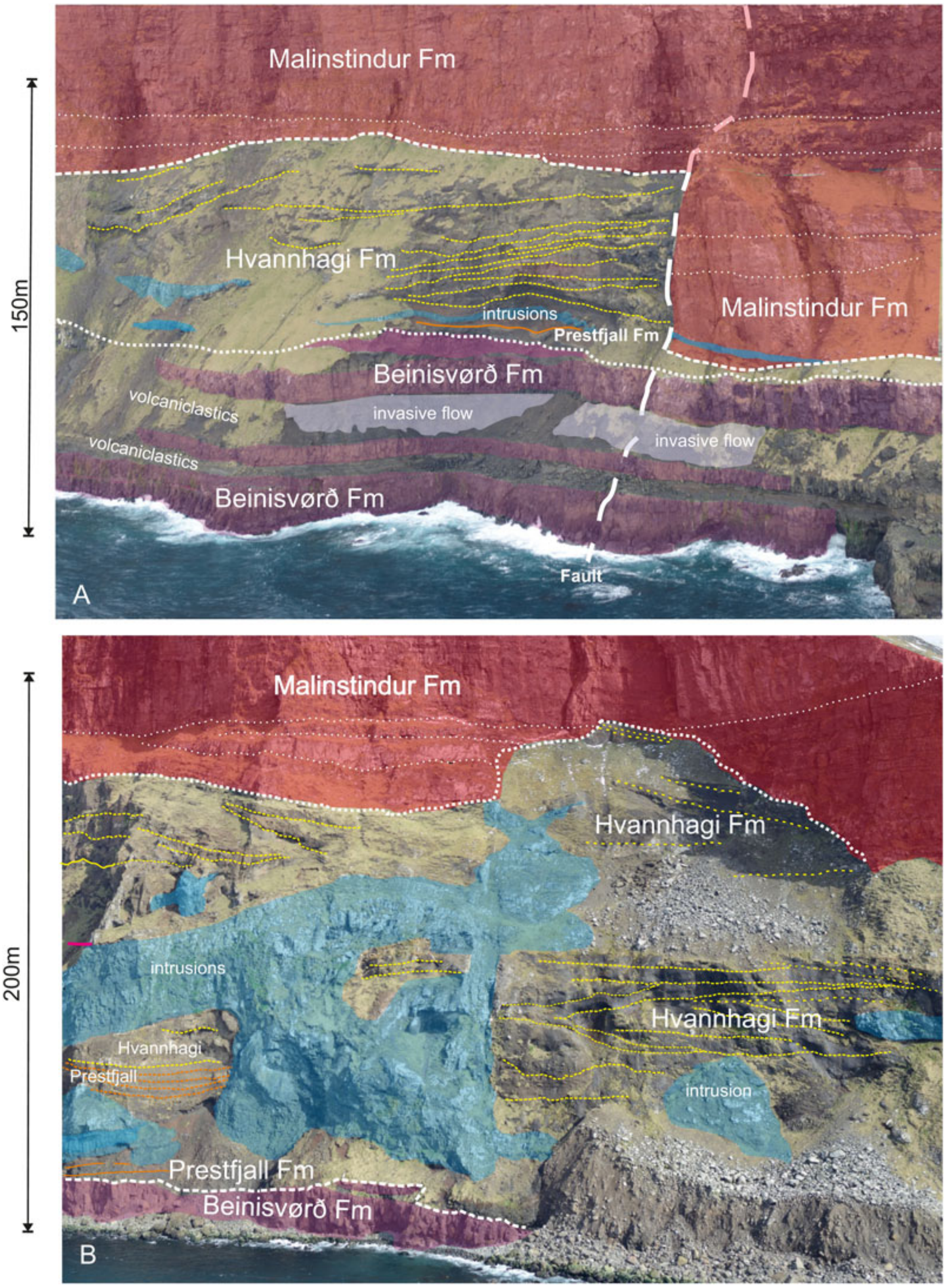


**Figure 14** (a) Interpreted photograph of the cliff exposure at Reyðastíggjatangi, south of Gásadalur; see Fig. 12a for location. Note the Malinstindur Formation lava flows have filled an eroded channel, the northern limit of which is defined by a strike slip fault; and (b) interpreted photograph of cliff exposures north of Bøur showing extensive intrusion of the volcaniclastic sedimentary rocks by basalt sills. The upper limit of the Hvannhagi Formation was clearly subjected to significant erosion before the emplacement of the overlying Malinstidur Formation flows. This is particularly notable to the left of the photograph, where thin bedded compound Malinstindur Formation flows fill a 'mini basin' in the top of the Hvannhagi Formation.

that erupted the late-stage simple lava flows. Ash, scoria, and weathered basalt clasts from the fissure zone would have been remobilised by rainfall and transported by hyperconcentrated flow as a muddy slurry (*cf.* Smith & Lowe 1991; Zernack 2021). These muddy lahars progressively infilled a pre-existing low, previously a zone of lava–water interaction south of Gásadalur village. The occurrence and thickness of these volcaniclastic deposits is clearly not related to the duration between eruptions (Millett *et al.* 2020). Their stratigraphical and paleogeographical location is instead a depositional system response to the presence of a substantial low-angle shield volcano to the northwest.

Despite the topographical annealing effect of the late-stage Beinisvørð Formation simple lava flows and interbedded lahar deposits, the geometry of the succeeding Prestfjall and Hvannhagi formations indicates persistence of a paleovalley in the Gásadalur to Bøur area. In the area of Tindhólmur, the Prestfjall Formation depositional system occupied a topographical low to the east of successive Beinisvørð Formation simple lava flow terminations. The finely bedded volcaniclastic sandstones of the Prestfjall Formation exposed on Tindhólmur (Fig. 9b) indicate deposition of volcaniclastic sediment in a localised lacustrine basin. This contrasts with the Prestfjall Formation fluvial sandstone/shale deposits drilled in the Gásadalur 1989-1 borehole

https://doi.org/10.1017/S1755691022000056 Published online by Cambridge University Press

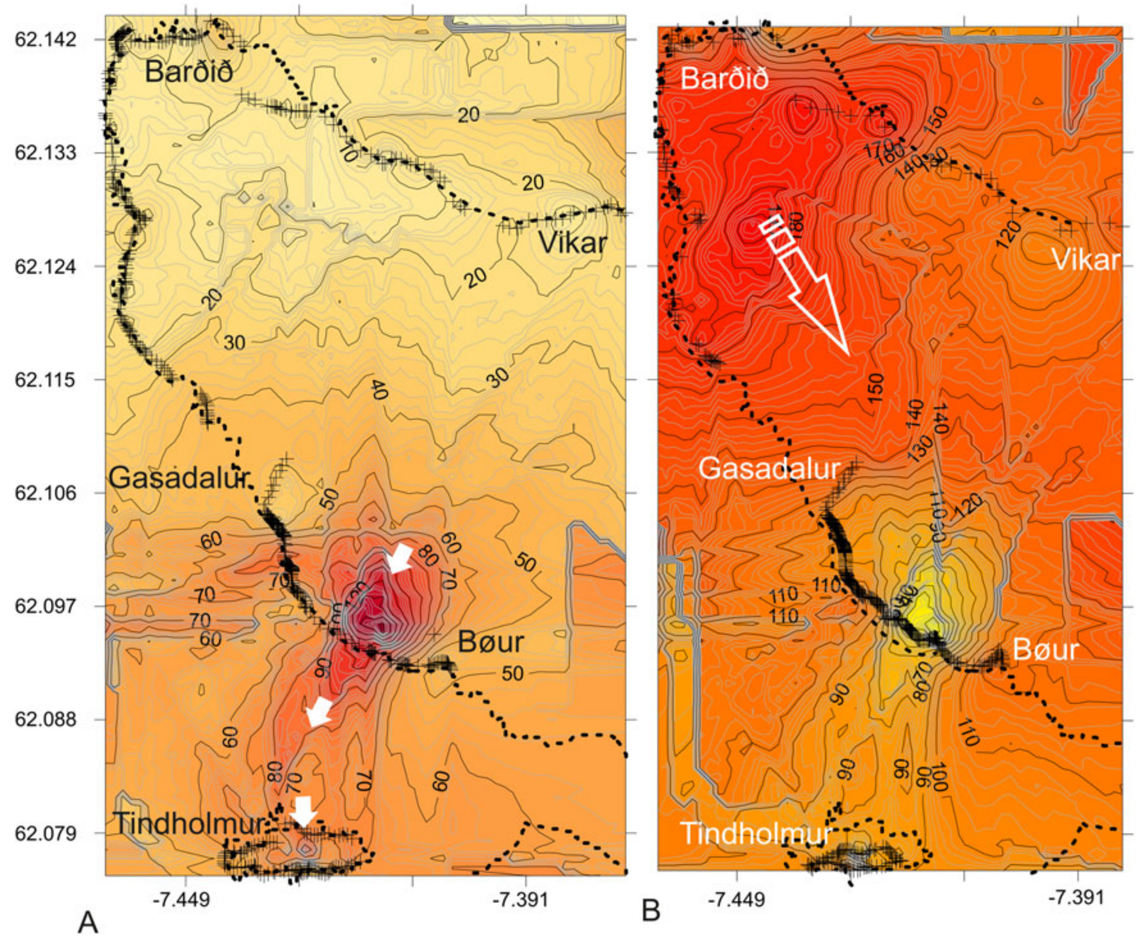


**Figure 15** Both Fig. 15a and 15b have isopach maps contoured in metres, and differential shading is used to highlight the contours with the most intense shading used for the thickest strata. (a) Isopach map of the combined thickness of the Prestfjall and Hvannhagi formations in the Vágar and Tindhólmur area. The south southwest trending main thickness of the Hvannhagi lahar turns more to the south at Tindhólmur (shown by the white arrows), following the trend recorded in the photogrammetry model (Fig. 8). Sourced from a reworked volcanic debris avalanche, the lahars originated north of Vágar. Note that because of post-Hvannhagi Formation erosion evident in Figs 12 and 14, the depositional thickness of the upper beds of the Hvannhagi Formation was significantly reduced. (b) The isopach of the overlying basal lava flows of the Malinstindur Formation highlights the trend of the lahar system, even allowing for post-depositional erosion. This map indicates that the low-angle shield producing these compound lavas lay to the north northwest off the north coast of Vágar. The sector collapse that sourced the lahars probably subcrops beneath thick Malinstindur lava flows to the northwest of Vágar.

and exposed within the Gásadalur to Bøur paleovalley, indicating a source of remobilised volcanic ash from a primary volcanic accumulation.

No lithological change is apparent in the Prestfjall Formation on Tindhólmur, but the blocky claystones at the top of the formation in the Gásadalur 1989-1 borehole contain evidence of a tidally influenced fluvial channel and a link to a source of extra-basinal clastic reworking. Several rises in relative sea level have been recorded within the FIBG lava pile (Jolley *et al.* 2012), potentially linked to drowning of the low-lying basalt plain in response to thermal subsidence at the cessation of Beinisvørð Formation eruption (Millett *et al.* 2020). This would have resulted in the formation of ria-like drowned valleys rather than sheet flooding of the basalt plain (Shaw Champion *et al.* 2008; Jolley *et al.* 2012, 2021).

The 150 m thick conglomeratic succession of the Hvannhagi Formation on Vágar is interpreted as a sequence of lahar deposits derived from remobilisation of a sector collapse volcanic debris avalanche (VDA) in the northwest of Vágar. Evidence of a VDA source for the Hvannhagi Formation on Vágar is provided by the high volume of very poorly sorted basalt clasts, derived from multiple lava flows. These VDA deposits were reworked as dilute lahars (*cf.* Zernack 2021) down the pre-existing valley system (Figs 12, 14–16). Repeated beds of very poorly sorted, unstructured to faintly bedded, and normally graded conglomerates indicate deposition under hyperconcentrated flow. Horizontally bedded sandstone units deposited in transition to fluvial flow occur in some units, suggesting dilution of the hyperconcentrated flow front, waning lahar states, or as lateral overbank facies. Further down the drainage slope at Tindhólmur, lahars initially deposited debris flow conglomerates. Here, waning flow resulted in the deposition of cross-bedded sandstones and pebbly sandstones showing transition from hyperconcentrated to streamflow (Fig. 9).

Considered by previous authors to be a transitional contact between the volcaniclastic deposits and compound lava flow field (Rasmussen & Noe-Nygaard 1970; Waagstein 1988; Passey & Jolley 2009), new photogrammetry data of the Hvannhagi–Malinstindur Unconformity indicate a more nuanced relationship. This unconformity marked a significant relative uplift event associated with dominantly strike-slip faulting both on Vágar and Tindhólmur. Faulting and erosion occurred along the fault scarp associated with erosion of a significant proportion of the upper Hvannhagi Formation, leaving an irregularly eroded topography of 119 m on Vágar. On Tindhólmur this relationship is seen to be more complex. Erosion of valley features and their subsequent partial infilling by basalt lava flows, was followed by a hiatus reflected in weathering of the central valley fill lavas. Subsequent deposition of the Hvannhagi Formation conglomerates was, in turn, followed by a rejuvenation of the central valley, with Malinstindur Formation compound lavas filling the central valley and onlapping the surrounding topography

https://doi.org/10.1017/S1755691022000056 Published online by Cambridge University Press

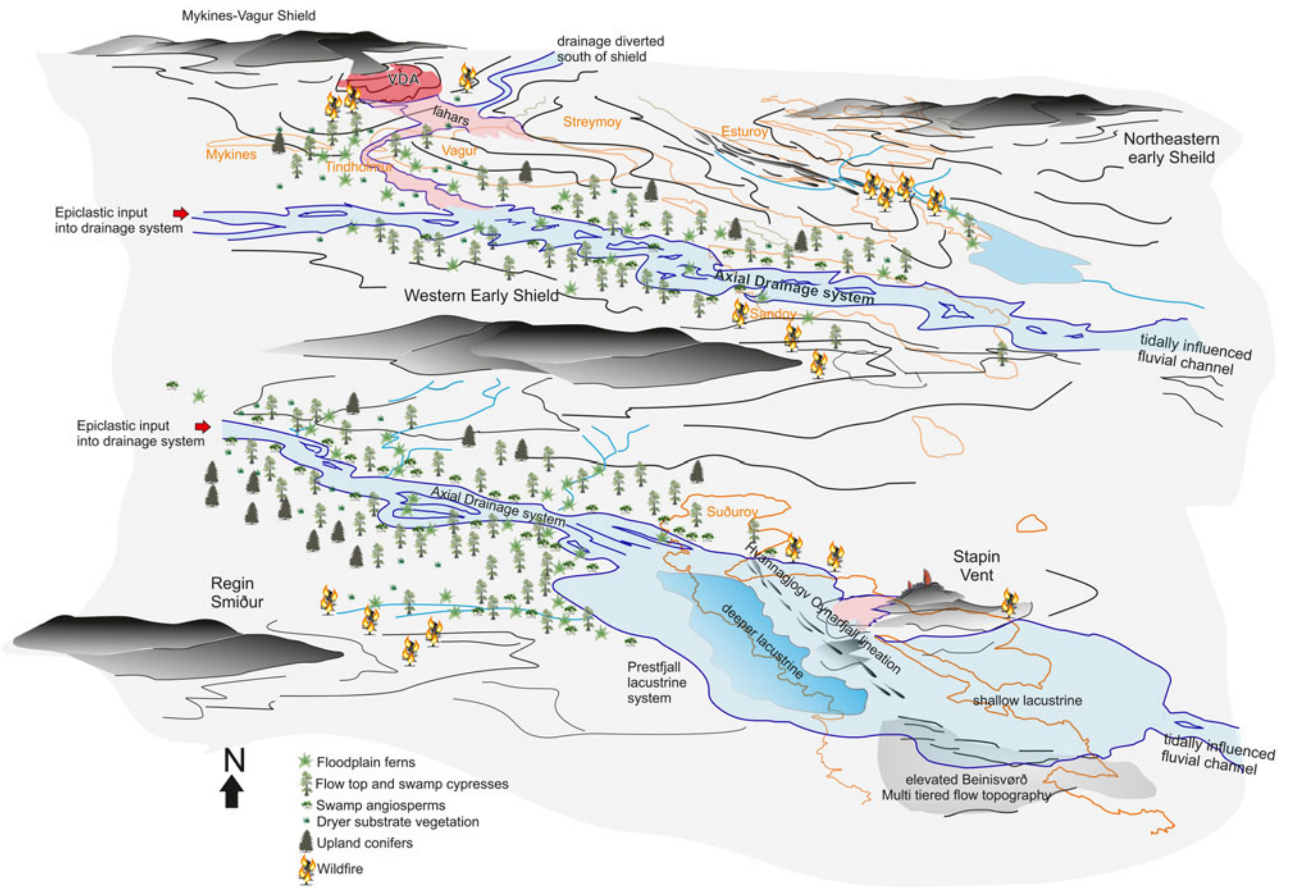


**Figure 16** Schematic perspective view of the Faroe Islands region at the onset of Hvannhagi Formation eruptive activity. The current island geography is outlined in orange. Large expanses of basalt plains topography were transected by drainage systems depositing volcaniclastic sedimentary beds. The position of these axial drainage systems was controlled by the end Beinisvørð Formation surface topography, faulting and active low-angle shield volcanoes. In the northwest, a volcanic debris avalanche (VDA, dark pink shading) sourced from a sector collapse on the Mykines–Vágar low-angle shield was reworked as lahar deposits into the drainage system. Similar localised lahar deposits and ashfall was sourced from a rejuvinated Stapin Vent on Suðuroy to the south. Drainage systems in valleys between low-angle shield volcanoes hosted the majority of the vegetation, high moisture demand swamp communitites being proximal to water courses and lacustrine zones.

(Figs 8, 10). This relationship confirms that eruption of lava flows characteristic of the Malinstindur Formation began following Prestfjall Formation deposition, prior to the VDA and associated lahar deposits of the Hvannhagi Formation in the north of the islands. The volcaniclastic deposits of the Hvannhagi Formation therefore represent dynamic, landscape scale events within the early Malinstindur Formation lava field.

Mapping of the basal Malinstindur Formation lava flow package (Fig. 15), illustrates that the flow field originated to the northwest, indicating continued eruptive activity sourced from the Mykines–Vágar shield. Subsequent basalt plains eruptions drowned the complex erosional topography of the Hvannhagi–Malinstindur Unconformity. The eroded surface of the upper Hvannhagi Formation created a series of 'mini-basins' which were the last to be overstepped by the compound flow field.

## 5.2. Suðuroy

A thick succession of eastwards dipping Beinisvørð Formation simple lava flows is exposed on the west coast of Suðuroy. These are regarded as having been sourced from an eruptive fissure system west of Suðuroy (Waagstein 1988; Passey & Varming 2010). Consequently, late Beinisvørð Formation lava flows and sedimentary rock interbeds vary in composition and thickness west to east across the island. Typical of this are the ponded columnar jointed (e.g., Kulagjógv Flow) and multi-tiered (e.g., Hov Flow) lava flows exposed in the interior of the island and north of Hov, respectively (Rasmussen & Noe-Nygaard 1970). These flows are not present on the west coast, being ponded down the depositional slope to the east. Similarly, interbedded volcanic debris flow units (e.g., at Hov) and volcaniclastic shale units (e.g., at Froðba) are recorded between lava flows in the east of the island (Fig. 1), but not seen in the west.

Vent proximal volcanic and volcaniclastic deposits occur in the northeast of Suðuroy, sourced from the Stapin Vent (Rasmussen & Noe-Nygaard 1970; Passey & Jolley 2009). The pyroclastic deposits of this vent form an annular structure, which elevated the area above the surrounding Beinisvørð Formation surface, a topography inherited during deposition of the Prestfjall Formation. Exposures inland are limited, but photogrammetry interpretation of the west coast has shown no evidence of significant erosion at the base of the Prestfjall Formation (Passey *et al.* 2016). As a consequence of this, deposition of the Suðuroy Prestfjall Formation lacustrine system was controlled by this landscape inheritance. Within the lacustrine Prestfjall Formation, repeated cycles in palynofloral ecology, geochemical ratios, and sedimentology, indicate that longer duration environmental forcing occurred (Fig. 6). There is no evidence that these cycles were related to lava field processes, but rather that they reflect orbital or solar forcing controlling lacustrine water depth via precipitation. Assuming 21 k obliquity or 40 ky eccentricity cycling (Berger 1988), this would indicate that the lacustrine record is 105–205 ky in duration.

Lateral facies variation between the uppermost units of the Prestfjall Formation and the basal Hvannhagi Formation/Malinstindur Formation is suggested by palynological data from Stapin, fossil wood in the lowermost Hvannhagi tuffs at Holið í Helli, and raised residual MgO values in the upper

https://doi.org/10.1017/S1755691022000056 Published online by Cambridge University Press

Prestfjall Formation of the KOLBHI-04 borehole. Incised channels filled with normally graded conglomerates and sandstones are linked here to overbank reddened clay stones which indicate localised erosion following deposition of the Prestfjall Formation in northwest Suðuroy. Elsewhere, the Prestfjall Formation is overlain by apparently conformably bedded volcanic, or thin volcaniclastic rocks of the Hvannhagi and Malinstindur formations.

The syn-eruptive facies of the Hvannhagi Formation on Suðuroy include primary pyroclastic tuffs, conglomerates, sandstones, and shales. These, primary olivine-phyric and welded tuffs confirm the linkage between the Hvannhagi Formation and the olivine-phyric lavas of the basal Malinstindur Formation (Rasmussen & Noe-Nygaard 1970; Hald & Waagstein 1984; Waagstein 1988; Larsen *et al.* 1999; Passey & Jolley 2009).

Exposures of the base of the Malinstindur Formation are infrequent on Suðuroy, and they are often poor or invaded by numerous dolerite sills. Previous authors (Rasmussen & Noe-Nygaard 1970; Waagstein 1988; Passey & Jolley 2009) identified a transitional zone where lower Malinstindur Formation lava flow lobes are interbedded with volcaniclastic rocks attributed to the Hvannhagi Formation. This is supported by the succession recorded in the KOLBH1-04 borehole, where these volcaniclastic interbeds occur in the Malinstindur Formation above the Hvannhagi Formation.

## 6. Conclusions

The Hvannhagi Formation of the FIBG is a rare deep time example of a sector collapse-generated debris flow deposit associated with a low-angle shield (3–5° slope). Many recorded modern and deep time examples are from more steeply sloped stratovolcanoes in continental settings, dissimilar to the Paleogene rifting margin of the northeast Atlantic (Waresback & Turbeville 1990; Smith 1991; Smith & Lowe 1991; Dufresne *et al.* 2021; Zernack 2021). Thick lahar successions in western Vágar were deposited in two main phases, isopach mapping indicating an origin up to >40 km north of the lahar deposits (Fig. 15; Cronin *et al.* 2000). These lahars were partly confined to a shallow north northeast–south southwest orientated topographical low, reflecting continued influence of late Beinisvørð Formation topography. A synchronous vent structure (a Malinstindur Formation rejuvenated Stapin Vent) northeast of Suðuroy (Fig. 16) sourced volcaniclastic deposits from pyroclastic eruptions. These eruptions initiated before the termination of Prestfjall Formation lacustrine shale deposition, suggesting that volcanism slowed considerably at the end of Beinisvørð Formation eruption, but did not stop completely.

The depositional geometries of the Hvannhagi Formation across the Faroe Islands exhibited no overriding single controlling factor. Proximity to volcanogenic source and eruptive morphologies interacted with syn-eruptive brittle fracturing and the inherited Beinisvørð–Prestfjall Unconformity surface to create a complex topography. This constrained debris flows, fluvial channels, and the interdigitating, onlapping lava flows of the Malinstindur Formation. The role of low-angle shield volcanoes in constraining the architecture and facies of sedimentary depositional systems is shown clearly. This study also highlights for the first time that shield volcanoes were coeval with and responsible for eruption of part of the Beinisvørð Formation, previously regarded as being composed solely of simple lava flows sourced from fissure erruptions (Passey & Bell. 2007; Passey & Jolley 2009). Exposures on Vágar and Mykines confirm the presence of a low-angle shield to the north which was previously identified from gravity data. Additional Beinisvørð Formation compound flow fields sourced from low-angle shields may exist beneath the extensive cover of later fissure sourced simple flows. This field observation also implies that the dominantly simple flow characteristic of the exposed Beinisvørð Formation is attributable to it being distal to eruption source.

The oldest volcaniclastic strata of the Hvannhagi Formation exposed in northeast Suðuroy are shown to be partly laterally equivalent to the upper beds of the Prestfjall Formation. Hvannhagi Formation volcaniclastic units subsequently also interdigitated with the prograding Malinstindur Formation compound flow field (Rasmussen & Noe-Nygaard 1970; Passey & Jolley 2009). To the north, eruption of localised Malinstindur Formation compound lava flows is recorded in topographical lows prior to deposition of the Hvannhagi Formation on Tindhólmur. The lack of widespread erosion at the base of the Prestfjall Formation and the diachronism of the Prestfjall–Hvannhagi and Hvannhagi–Malinstindur formations' boundaries all indicate a broad continuum of depositon and eruption. The pre-rift to syn-rift transition represented by the Beinisvørð to Malinstindur formations interval is stratigraphically equivalent to the the Flett Unconformity recorded on the eastern margin of the Faroe–Shetland Basin (Shaw Champion *et al.* 2008; Hartley *et al.* 2011; Jolley *et al.* 2021). This major unconformity rejuvenated the earlier Upper Thanetian Unconformity surface, resulting in the incision of basin-facing dendritic draininge systems in response to rift flank uplift. Within the stratigraphically equivalent Beinisvørð to Malinstindur formations interval, there are complex facies changes between lava flow field, fluvial, lacustrine to primary volcaniclastic, and lahar. These deposits, while locally sculpted as part of a complex lava field terrain, reperesent the correlative conformity of the major Flett Unconformity.

Cessation of volcanism at the end of Beinisvørð Formation eruption in the FIBG area, was regarded as a response to a transient reduction in mantle temperature (Millett *et al.* 2020). The resultant volcanic hiatus is however, short or a period of very low eruption frequency less than the duration of Prestfjall Formation deposition. Characterised by sedimentary depositional systems, the eruptive hiatus or slow-down was followed by an initially episodic resumption of volcanism focussed on multiple low-angle shields. This style of volcanism replaced the fissure-fed and distal to source lava plain facies of the Beinisvørð Formation. It is this more varied, local sourcing that gives rise to the complex interactions of VDA's, lahars and pyroclastic deposits forming the Malinstindur Formation, and the interdigitation of these deposits with the uppermost Prestfjall Formation and oldest Malinstindur Formation lava flows.

## 7. Supplementary material

Supplementary material is available online at https://doi.org/10.1017/S1755691022000056

## 8. Acknowledgements

The photogrammetry survey for this study was carried out as part of the Cambridge Arctic Shelf Project (CASP)'s Flood Basalt Impact on Hydrocarbon Systems Project 2014–16 and CASP's sponsors' financial support is gratefully acknowledged as well as the Geological Survey of Denmark and Greenland' contribution. We would also like to thank Atlantic Airways for their help in the acquisition of the oblique photographs used in preparation and interpretation of the models. Davie Brown and an anonymous reviewer are thanked for helpful reviews of the manuscript. John Howell is thanked for discussions on photogrammetry and decompaction of the sedimentary rock record.

https://doi.org/10.1017/S1755691022000056 Published online by Cambridge University Press

## 9. References


Anderson, J. T. 1998. The effect of seasonal variability on the germination and vertical transport of a cyst forming dinoflagellate, *Gyrodinium* sp., in the Chesapeake Bay. *Ecological Modelling* **112**, 85–109.

Berger, A. 1988. Milankovitch theory and climate. *Reviews of Geophysics* **26**, 624–57.

Bjørlykke, K., Jahren, J., Mondol, N. H., Marcussen, O., Croize, D., Peltonen, C. & Thyberg, B. 2009. *Sediment compaction and rock properties.* AAPG International Conference and Exhibition, 26–29 October 2008, Cape Town, South Africa, Search and Discovery Article 50192.

Buckley, S. J., Ringdal, K., Naumann, N., Dolva, B., Kurz, T. H., Howell, J. A. & Dewez, T. J. B. 2019. LIME: software for 3-D visualization, interpretation, and communication of virtual geoscience models. *Geosphere* **15**, 222–35.

Bujak, J. P., Downie, C., Eaton, G. L. & Williams, G. L. 1980. Dinoflagellate cysts and acritarchs from the Eocene of southern England. *Palaeontological Association, Special Papers in Palaeontology* **24**, 1–100.

Chaney, R. W. 1951. A revision of fossil *Sequoia* and *Taxodium* in western North America based on the recent discovery of *Metasequoia*. *Transactions of the American Philosophical Society* **40**, 171–263.

Chapin, F. S. I. I. I., Walker, L. R., Fastie, C. L. & Sharman, L. C. 1994. Mechanisms of primary succession following deglaciation at Glacier Bay, Alaska. *Ecological Monographs* **64**, 149–75.

Collinson, M. E. 2002. The ecology of Cainozoic ferns. *Review of Palaeobotany and Palynology* **119**, 51–68.

Cronin, S. J., Lecointre, J. A., Palmer, A. S. & Neall, V. E. 2000. Transformation, internal stratification, and depositional processes within a channelised, multi-peaked lahar flow. *New Zealand Journal of Geology and Geophysics* **43**, 117–28.

Daly, R. J., Jolley, D. W., Spicer, R. A. & Ahlberg, A. 2011a. A palynological study of an extinct Arctic ecosystem from the Palaeocene of northern Alaska. *Review of Palaeobotany and Palynology* **166**, 107–16.

Daly, R. J., Jolley, D. W., Spicer, R. A. & Ahlberg, A. 2011b. The role of angiosperms in Palaeocene Arctic ecosystems: a palynological study from the Alaskan North Slope. *Palaeogeography, Palaeoclimatology, Palaeoecology* **309**, 374–82.

Debenay, J. P., Carbonel, P., Morzadec-Kerfourn, M.-T., Cazaubon, A., Denèfle, M. & Lézine, A.-M. 2003. Multi-bioindicator study of a small estuary in Vendée (France). *Estuarine, Coastal and Shelf Science* **58**, 843–60.

Dufresne, A., Siebert, L. & Bernard, B. 2021. Distribution and geometric parameters of volcanic debris avalanche deposits. In: Roverato, M., Dufresne, A. & Procter, J. (eds) *Volcanic debris avalanches. From collapse to hazard. Advances in volcanology*, 75–90. Cham, Switzerland: Springer.

Elliott, R. E. 1984. Quantification of peat to coal compaction stages, based especially on phenomena in the East Pennine Coalfield, England. *Proceedings of the Yorkshire Geological Society* **45**, 163–72.

Ellis, D., Jolley, D. W., Passey, S. R. Bell, B. R. 2009. Transfer Zones: The application of new geological information from the Faroe Islands to the offshore exploration of intra basalt and sub basalt prospects. In: Varming, T. *et al.* (eds.) *Faroe Islands Exploration Conference: Proceedings of the 2nd Conference*, Tórshavn, 205–26.

Hald, N. & Waagstein, R. 1984. Lithology and chemistry of a 2-km sequence of Lower Tertiary tholeiitic lavas drilled on Suðuroy, Faeroe Islands (Lopra-1). In: Berthelsen, O., Noe-Nygaard, A. & Rasmussen, J. (eds.) *The Deep Drilling Project 1980–1981 in the Faeroe Islands.* Annales Societatis Scientiarum Færoensis, Tórshavn, Supplementum IX, 15–38.

Hartley, R. A., Roberts, G. C., White, N. & Richardson, C. 2011. Transient convective uplift of an ancient buried landscape. *Nature Geoscience* **4**, 562–5.

Hobbie, E. A., Macko, S. A. & Shugart, H. H. 1998. Patterns in N dynamics and N isotopes during primary succession. *Chemical Geology* **152**, 3–11.

Jolley, D. W. 1997. Palaeosurface palynofloras of the Skye lava field and the age of the British Tertiary Volcanic Province. In: Widdowson, M. (ed.) *Palaeosurfaces: recognition, reconstruction and palaeoenvironmental interpretation*, vol. **120**. Geological Society, 67–94. London, Special Publications.

Jolley, D. W., Bell, B. R., Williamson, I. T. & Prince, I. 2009. Syn-eruption vegetation dynamics, paleosurfaces and structural controls on lava field vegetation: an example from the Palaeogene Staffa Formation, Mull Lava Field, Scotland. *Review of Palaeobotany and Palynology* **153**, 19–33.

Jolley, D. W., Gilmour, I., Gilmour, M., Kemp, D. B. & Kelley, S. P. 2015. Long-term resilience decline in plant ecosystems across the Danian Dan-C2 hyperthermal event, Boltysh crater, Ukraine. *Journal of the Geological Society, London* **172**, 491–8.

Jolley, D. W., Millett, J. M., Schofield, N., Broadley, L. & Hole, M. J. 2021. Stratigraphy of volcanic rock successions of the North Atlantic rifted margin: the offshore record of the Faroe–Shetland and Rockall basins. *Earth and Environmental Science Transactions of the Royal Society of Edinburgh*. Online First. https://doi.org/10.1017/S1755691021000037.

Jolley, D. W. & Morton, A. C. 1992. Palynological and petrological characterisation of a North Sea volcaniclastic sequence. *Proceedings of the Geologists' Association* **103**, 119–27.

Jolley, D. W., Passey, S. R., Hole, M. & Millett, J. 2012. Large-scale magmatic pulses drive plant ecosystem dynamics. *Journal of the Geological Society, London* **169**, 703–11.

Jolley, D. W., Widdowson, M. & Self, S. 2008. Volcanogenic nutrient fluxes and plant ecosystems in large igneous provinces: an example from the Columbia River Basalt Group. *Journal of the Geological Society, London* **165**, 955–66.

Knox, R. W. O. B. & Morton, A. C. 1988. The record of early Tertiary N Atlantic volcanism in sediments of the North Sea Basin. In: Morton, A. C. & Parson, L. M. (eds) *Early Tertiary volcanism and the opening of the NE Atlantic*, vol. **39**. Geological Society, 407–19. London: Special Publications.

Larsen, L. M., Waagstein, R., Pedersen, A. K. & Storey, M. 1999. Trans-Atlantic correlation of the Palaeogene volcanic successions in the Faeroe Islands and East Greenland. *Journal of the Geological Society, London* **156**, 1081–95.

Lund, J. 1983. Biostratigraphy of interbasaltic coals from the Faeroe Islands. In: Bott, M.H.P., Saxov, S., Talwani, M. & Thiede, J. (eds) *Structure and development of the Greenland–Scotland Ridge: New methods and concepts*, 417–23. New York, Plenum Press.

Lund, J. 1989. A late Paleocene non-marine microflora from the interbasaltic coals of the Faeroe Islands, North Atlantic. *Bulletin of the Geological Society of Denmark* **37**, 181–203.

Millett, J. M., Hole, M. J., Jolley, D. W., Passey, S. R. & Rossetti, L. 2020. Transient mantle cooling linked to regional volcanic shut-down and early rifting in the North Atlantic Igneous Province. *Bulletin of Volcanology* **82**, 10.1007/s00445-020-01401-8.

Mondol, N. H., Bjørlykke, K., Jahren, J. & Høeg, K. 2007. Experimental mechanical compaction of clay mineral aggregates—changes in physical properties of mudstones during burial. *Marine and Petroleum Geology* **24**, 289–311.

Newberry, J. S. 1863. Descriptions of fossil plants collected by Mr. George Gibbs. *Boston Journal of Natural History* **7**, 506–25.

Parra, M., Delmont, P., Dumon, J. C., Ferragne, A. & Pons, J. C. 1987. Mineralogy and origin of Tertiary interbasaltic clays from the Faeroe Islands, northeastern Atlantic. *Clay Minerals* **22**, 63–82.

Passey, S. R. 2004. *The volcanic and sedimentary evolution of the Faeroe Plateau Lava Group, Faeroe Islands and the Faeroe–Shetland Basin, NE Atlantic*. PhD Thesis, University of Glasgow, 450 pp.

Passey, S. R. 2014. The habit and origin of siderite spherules in the Eocene coal-bearing Prestfjall Formation, Faroe Islands. *International Journal of Coal Geology* **122**, 76–90.

Passey, S. R. & Bell, B. R. 2007. Morphologies and emplacement mechanisms of the lava flows of the Faroe Islands Basalt Group, Faroe Islands, NE Atlantic Ocean. *Bulletin of Volcanology* **70**, 139–56.

Passey, S. R. & Jolley, D. W. 2009. A revised lithostratigraphic nomenclature for the Palaeogene Faroe Islands Basalt Group, NE Atlantic Ocean. *Earth and Environmental Science Transactions of the Royal Society of Edinburgh* **99**, 127–58.

Passey, S. R. & Varming, T. 2010. Surface interpolation within a continental flood basalt province: an example from the Palaeogene Faroe Islands Basalt Group. *Journal of Structural Geology* **32**, 709–23.

Passey, S. R., Vosgerau, H., Sørensen, E. V. & Vautravers, B. P. H. 2016. *Photogrammetric study of the volcanic cliff sections of western Suðuroy, Faroe Islands and their implications for hydrocarbon exploration*. CASP, Cambridge, CASP.FBP2014–16.9, p. 128.

Pierson, T. C., Pringle, P. T. & Cameron, K. A. 2011. Magnitude and timing of downstream channel aggradation and degradation in response to a dome-building eruption at Mount Hood, Oregon. *Geological Society of America Bulletin* **123**, 3–20.

Pross, J. & Brinkhuis, H. 2005. Organic-walled dinoflagellate cysts as peleoenvironmental incicators in the Paleogene; a synopsis of concepts. *Paläontologische Zeitschrift* **79/1**, 53–9.

Rasmussen, J. & Noe-Nygaard, A. 1970 (1969). *Geology of the Faeroe Islands* (*Pre-Quaternary*). *Trans:* Henderson, G. Geological Survey of Denmark, Copenhagen, 1/25, p. 142.

Retallack, G. J. 1999. Post-apocalyptic greenhouse paleoclimate revealed by earliest Triassic paleosols in the Sydney Basin, Australia. *Geological Society of America Bulletin* **111**, 52–70.

Schofield, N., Heaton, L., Holford, S. P., Archer, S. G., Jackson, C. A.-L. & Jolley, D. W. 2012. Seismic imaging of 'broken bridges': linking seismic to outcrop-scale investigations of intrusive magma lobes. *Journal of the Geological Society, London* **169**, 421–6.

Schrøder, N. F. 1971. Magnetic anomalies around the Faeroe Islands. *Fróðskaparrit* **19**, 20–9.

Shaw Champion, M. E., White, N. J., Jones, S. M. & Lovell, J. P. B. 2008. Quantifying transient mantle convective uplift: an example from the Faroe–Shetland Basin. *Tectonics* **27**, TC1002. doi: 10.129/2007TC002106

Sheldon, N. D. 2003. Pedogenesis and geochemical alteration of the picture gorge subgroup, Columbia River Basalt, Oregon. *Geological Society of America Bulletin* **115**, 1377–87.

Sheldon, N. D. & Tabor, N. J. 2009. Quantitative paleoenvironmental and paleoclimatic reconstructions using paleosols. *Earth Science Reviews* **95**, 1–52.

Smith, G. A. 1991. Facies sequences and geometries in continental volcaniclastic sediments. In: Fisher, R.V. & Smith, G. A. (eds.) *Sedimentation in volcanic settings*, vol. **45**, 109–21. Broken Arrow, OK, USA: SEPM Special Publication.

Smith, G. A. & Lowe, D. R. 1991. Lahars: volcano-hydrologic events and deposition in the debris flow-hyperconcentrated flow continuum. In: Fisher, R.V. & Smith, G.A. (eds.) *Sedimentation in volcanic settings*, vol. **45**, 59–70. Broken Arrow, OK, USA: SEPM Special Publication.

Sørensen, E. V. & Dueholm, M. 2018. Analytical procedures for 3D mapping at the photogeological laboratory of the Geological Survey of Denmark and Greenland. *GEUS Bulletin* **41**, 99–104.

Striegler, U. 1990. Paleobotanical studies in lower Lusatia. In: Knobloch, E. & Kvacek, Z. (eds) *Proceedings of the Symposium Palaeofloristic and Paleoclimatic Changes in the Cretaceous and Tertiary.* Geological Survey, Prague, pp. 233–8.

Tappan, H. 1980. *Paleobiology of the protists.* San Francisco: Freeman & Company, W. H., 1028 pp.

Thornton, I. W. B. 2000. The ecology of volcanoes: recovery and reassembly of living communities. In: Sigurdsson, H. (ed.) *Encyclopedia of volcanoes*, 1057–81. New York: Academic Press.

Vieira, M. & Jolley, D. 2020. Stratigraphic and spatial distribution of palynomorphs in deep-water turbidites: a meta-data study from the UK central North Sea Paleogene. *Marine & Petroleum Geology* **122**, 104638.

Vitousek, P. M. 2004. *Nutrient cycling and limitation: Hawai'i as a model system*. Princeton, NJ: Princeton University Press.

Vosgerau, H., Passey, S. R., Svennevig, K., Strunck, M. N. & Jolley, D. W. 2016. Reservoir architectures of interlava systems - a 3D photogrammetrical study of Eocene cliff sections, Faroe Islands. In: Bowman, M., Smyth, H. R., Good, T. R., Passey, S. R., Hirst, J. P. P. & Jordan, C. J. (eds) *The value of outcrop studies in reducing subsurface uncertainty and risk in hydrocarbon exploration and production*, vol. **436**. Geological Society, 55–73. London: Special Publications.

Waagstein, R. 1988. Structure, composition and age of the Faeroe Basalt Plateau. In: Morton, A. C. & Parson, L. M. (eds) *Early Tertiary volcanism and the opening of the NE Atlantic*, vol. **39**. Geological Society, 225–38. London: Special Publications.

Waresback, D. B. & Turbeville, B. N. 1990. Evolution of a Plio-Pleistocene volcanogenic-alluvial fan: the Puye Formation, Jemez Mountains, New Mexico. *Geological Society of America Bulletin* **102**, 298–314.

Whittaker, R. J., Bush, M. B. & Richards, K. 1989. Plant recolonization and vegetation succession on the Krakatau Islands, Indonesia. *Ecological Monographs* **59**, 59–123.

Wing, S. L. & Hickey, L. J. 1984. The *Platycarya* perplex and the evolution of the Juglandaceae. *American Journal of Botany* **71**, 388–411.

Zernack, A. V. 2021. Volcanic debris-avalanche deposits in the context of volcaniclastic ring plain successions - A case study from Mt. Taranaki. In: Roverato, M., Dufresne, A. & Procter, J. (eds) *Volcanic debris avalanches. From collapse to hazard. Advances in volcanology*, 211–54. Cham, Switzerland: Springer.

MS received 15 October 2021. Accepted for publication 21 March 2022. First published online 19 April 2022

https://doi.org/10.1017/S1755691022000056 Published online by Cambridge University Press